Title

A missense point mutation in nerve growth factor (NGF^{R100W}) results in selective peripheral sensory neuropathy.

Authors

Yang, Wanlin
Sung, Kijung
Xu, Wei
et al.

Publication Date

2020-11-01

DOI

10.1016/j.pneurobio.2020.101886

Progress in Neurobiology 194 (2020) 101886

Contents lists available at ScienceDirect

Progress in Neurobiology

journal homepage: www.elsevier.com/locate/pneurobio

Original Research Article

A missense point mutation in nerve growth factor (NGF^{R100W}) results in selective peripheral sensory neuropathy

Wanlin Yang[a,b,c,1], Kijung Sung[b,1], Wei Xu[a], Maria J Rodriguez[b,d], Andrew C. Wu[b], Sarai A. Santos[b], Savannah Fang[b], Rebecca K. Uber[b], Stephanie X. Dong[b], Brandon C. Guillory[b], Xavier Orain[b], Jordan Raus[b], Corrine Jolivalt[d], Nigel Calcutt[d], Robert A. Rissman[b,e], Jianqing Ding[a], Chengbiao Wu[b,*]

[a] Department of Neurology and Institute of Neurology, Ruijin Hospital, Shanghai Jiao Tong University School of Medicine, Shanghai, China
[b] Department of Neurosciences, University of California San Diego, La Jolla, CA, USA
[c] Department of Neurology, Zhuijiang Hospital, Southern Medical University, Guangzhou, China
[d] Department of Pathology, University of California San Diego, La Jolla, CA, USA
[e] Veterans Affairs San Diego Healthcare System, San Diego, CA, USA

ARTICLE INFO

Keywords:
Hereditary sensory autonomic neuropathy V
Knockin mouse model
Pain
Nerve growth factor
TrkA
p75 neutrophic factor receptor
Nociception
Cognition
Intraepidermal nerve fiber
Dorsal root ganglion

ABSTRACT

The R100W mutation in nerve growth factor is associated with hereditary sensory autonomic neuropathy V in a Swedish family. These patients develop severe loss of perception to deep pain but with apparently normal cognitive functions. To better understand the disease mechanism, we examined a knockin mouse model of HSAN V. The homozygous mice showed significant structural deficits in intra-epidermal nerve fibers (IENFs) at birth. These mice had a total loss of pain perception at ~2 months of age and often failed to survive to adulthood. Heterozygous mutant mice developed a progressive degeneration of small sensory fibers both behaviorally and functionally: they showed a progressive loss of IENFs starting at the age of 9 months accompanied with progressive loss of perception to painful stimuli such as noxious temperature. Quantitative analysis of lumbar 4/5 dorsal root ganglia revealed a significant reduction in small size neurons, while analysis of sciatic nerve fibers revealed the heterozygous mutant mice had no reduction in myelinated nerve fibers. Significantly, the amount of NGF secreted from mouse embryonic fibroblasts were reduced from both heterozygous and homozygous mice compared to their wild-type littermates. Interestingly, the heterozygous mice showed no apparent structural alteration in the brain: neither the anterior cingulate cortex nor the medial septum including NGF-dependent basal forebrain cholinergic neurons. Accordingly, these animals did not develop appreciable deficits in tests for brain function. Our study has thus demonstrated that the NGF^{R100W} mutation likely affects the structure and function of peripheral sensory neurons.

1. Introduction

Nerve growth factor (NGF) is a member of the neurotrophic factor family (NTF) that includes brain-derived neurotrophic factor (BDNF), neurotrophin 3 (NT-3) and neurotrophin 4 (NT-4) (Chao, 2003; Chao and Hempstead, 1995; Huang and Reichardt, 2001; Levi-Montalcini, 1987, 2004; Levi-Montalcini et al., 1995). These trophic factors act through two distinct receptors, Trk, the 140 kD tyrosine receptor kinase (TrkA for NGF; TrkB for BDNF, NT-3; TrkC for NT-4) and the 75 kD neurotrophin receptor ($p75^{NTR}$) to transmit signals in responsive neurons (Bothwell, 1995; Chao and Hempstead, 1995; Kaplan and Miller, 1997). The trophic function of NTFs is largely mediated by Trk, while $p75^{NTR}$ has a more diverse effects on survival, differentiation and death of neurons (Casaccia-Bonnefil et al., 1998; Chao and Hempstead, 1995; Nykjaer et al., 2005).

NGF exerts potent trophic actions on sensory and sympathetic neurons of the peripheral nervous system (PNS)(Hamburger and Levi-Montalcini, 1949) and also regulates the trophic status of striatal and basal forebrain cholinergic neurons (BFCNs) of the central nervous system (CNS)(Conover and Yancopoulos, 1997; Kew et al., 1996;

* Corresponding author at: Department of Neurosciences, University of California San Diego, Medical Teaching Facility, Room 312MC-0624, 9500 Gilman Drive, La Jolla, CA, 92093-0624, United States.
E-mail address: chw049@ucsd.edu (C. Wu).
[1] These authors contributed equally

https://doi.org/10.1016/j.pneurobio.2020.101886
Received 26 September 2019; Received in revised form 9 June 2020; Accepted 11 July 2020
Available online 18 July 2020
0301-0082/

Lehmann et al., 1999; Levi-Montalcini and Hamburger, 1951; Li and Jope, 1995; Svendsen et al., 1994). Given its robust trophic effects, NGF has been investigated for therapeutic properties for treating both PNS and CNS diseases. For example, NGF was explored for treating/preventing degeneration of BFCNs in Alzheimer's disease (AD) (Blesch and Tuszynski, 1995; Cuello et al., 2010; Eriksdotter Jonhagen et al., 1998; Hefti, 1994; Knusel and Gao, 1996; Koliatsos, 1996; Mufson et al., 2008; Olson, 1993; Rafii et al., 2014; Schindowski et al., 2008; Schulte-Herbruggen et al., 2008; Scott and Crutcher, 1994; Williams et al., 2006). However, some significant issues associated with administration of recombinant NGF such as back pain, injection site hyperalgesia, myalgia, weight loss led to the termination of these trials(Eriksdotter Jonhagen et al., 1998; Hefti, 1994; Knusel and Gao, 1996; Koliatsos, 1996; Olson, 1993; Scott and Crutcher, 1994). Other clinical efforts using NGF for treating diabetic neuropathies, HIV-induced peripheral neuropathies were also terminated due to the extreme side effects of pain(Apfel, 2002; Apfel et al., 1998; Hellweg and Hartung, 1990; Lein, 1995; McArthur et al., 2000; Pradat, 2003; Quasthoff and Hartung, 2001; Rask, 1999; Schifitto et al., 2001; Unger et al., 1998; Walwyn et al., 2006). These adverse effects such as severe pain associated with NGF administration has proven to be a significant roadblock for NGF-based therapies.

Indeed, NGF has also been recognized as a potent mediator of pain (Chuang et al., 2001; Lewin and Mendell, 1993; Lewin et al., 1993; Watanabe et al., 2008). This is further supported by genetic and clinical evidence demonstrating that both TrkA and $p75^{NTR}$-mediated signaling contributes to NGF-induced hyper-sensitization. For example, hereditary sensory and autonomic neuropathy type IV (HSAN IV) is resulted from recessive mutations in TrkA, these patients display pain insensitivity as well as mental retardation (Indo, 2001, 2002). Furthermore, many TrkA downstream effectors have also been implicated in NGF-mediated nociception: Pharmacological Inhibition of either the extracellular signal-regulated kinases (Erk) or phosphoinositide 3-kinase (PI3K) attenuates NGF-induced hyperalgesia (Zhang and Nicol, 2004). Activation of Phospholipase C (PLCγ) by NGF also potentiates nociceptive ion channels leading to hyperalgesia (Chuang et al., 2001). $p75^{NTR}$ is also involved in NGF-induced hyperalgesia. For example, injecting a $p75^{NTR}$ neutralizing antibody blocked NGF-induced hyperalgesia and NGF-mediated sensitization of action potentials in sensory neurons (Watanabe et al., 2008; Zhang and Nicol, 2004). Ceramide, a p75 downstream effector, is known to increase the number of action potentials in sensory neurons (Zhang et al., 2002, 2006). Nerve injury, axotomy, seizure, or ischemia can all cause an increase in both the expression and axonal transport of $p75^{NTR}$, thereby contributing to nociception (Zhou et al., 1996) (Roux et al., 1999). $p75^{NTR}$ downstream signaling cascades were responsible for mechanical hyperalgesia following NGF injection (Khodorova et al., 2013). Therefore, both TrkA and $p75^{NTR}$ receptor(s)-mediated signaling pathways play an important role in the pain signaling and function of NGF, although their relative contribution is yet to be defined.

The discovery of NGF mutations in human patients further highlights the importance of NGF in nociception. A homozygous mutation in the NGF gene [680C > A] + [681_682delGG] has been linked to hereditary sensory neuropathy in a consanguineous Arab family(Carvalho et al., 2011). Those affected individuals were completely unable to perceive pain, did not sweat, could not discriminate temperature (Carvalho et al., 2011). In addition, the patients had a chronic immunodeficiency and showed intellectual disabilities (Carvalho et al., 2011).

In a second case, a missense mutation in NGF (661C > T) was discovered in patients in consanguineous Swedish families who suffered from severe loss of deep pain, bone fractures and joint destruction (Einarsdottir et al., 2004). The disorder was classified as HSAN V (Online Mendelian Inheritance in Man (OMIM) # 608654). This particular mutation resulted in a substitution of tryptophan (W) for arginine (R) at Residue 211 in the proNGF polypeptide (pro-NGF^{R221W} that corresponds to Residue 100 in the mature protein: NGF^{R100W}) (Einarsdottir et al., 2004). The mutation is thus referred as NGF^{R100W} herein. Interestingly, unlike HSAN IV patients with recessive TrkA mutation(s) that develop pain insensitivity as well as mental retardation, HSAN V patients suffer from selective loss of pain sensation with normal cognitive function. This suggests that the NGF^{R100W} mutation causes selective loss of pain function, but likely retains intact trophic function (Einarsdottir et al., 2004; Minde et al., 2009, 2004; Minde, 2006; Perini et al., 2016; Sagafos et al., 2016). Therefore, NGF^{R100W} provides an important tool to uncouple the trophic function of NGF from its nociceptive actions (Capsoni, 2014; Capsoni et al., 2011; Cattaneo and Capsoni, 2019; Sung et al., 2018, 2019; Testa et al., 2019a; Yang et al., 2018).

Previous studies have revealed that the R100W mutation might disrupt the processing of proNGF to mature NGF (Larsson et al., 2009). We and others also examined the binding and signaling properties of the mature form of naturally occurring mutant NGF (NGF^{R100W}) and discovered that NGF^{R100W} retained its ability to bind to and signal through TrkA to induce trophic effects, but failed to bind or activate $p75^{NTR}$ (Covaceuszach et al., 2010; Sung et al., 2018). Consistent with these studies, NGF^{R100E} or $NGF^{P61SR100E}$ was also shown to be able to activate TrkA, but not $p75^{NTR}$ signaling (Capsoni et al., 2011; Covaceuszach et al., 2010). Together, these studies have provided strong support for a role of $p75^{NTR}$ in NGF-induced pain function. Failure to activate $p75^{NTR}$ signaling is likely a major reason for loss of pain in HSAN V patients (Capsoni, 2014; Capsoni et al., 2011; Cattaneo and Capsoni, 2019; Sung et al., 2018, 2019; Testa et al., 2019a,b; Yang et al., 2018).

HSAN V is an extremely rare disease that makes it impossible to perform systematic study of signaling mechanism and function of NGF^{R100W} in HSAN V patients. Given that NGF is highly conserved between mice and human, mouse models of HSAN V harboring NGF^{R100W} have provided an important vehicle to carefully examine the effects of NGF^{R100W} on development/ maintenance of both the central nervous system (CNS) and the peripheral nervous system (PNS) in vivo (Testa et al., 2019a; Yang et al., 2018). Using the knock-in mouse model of HSAN V that harboring the mouse NGF^{R100W} allele, we previously reported that mice carrying homozygous NGF^{R100W} alleles (fln/fln) displayed normal embryonic development of major organs (heart, lung, liver, kidney, and spleen) showed normal gene expression of either TrkA or $p75^{NTR}$ receptor (Yang et al., 2018). Interestingly, they exhibited extremely low counts of intra-epidermal nerve fibers (IENFs) at birth (Yang et al., 2018). In a recent study, Testa and colleagues have demonstrated that knocking in a human NGF allele carrying the R100W mutation resulted in a deficit in nociception but apparently with normal learning or memory (Testa et al., 2019b).

In the present study, we further characterized the impact of NGF^{R100W} on the structure and function of the brain and peripheral nervous system in the knock-in mouse model of HSAN V carrying mouse NGF^{R100W} mutation (Yang et al., 2018). We showed that unlike the homozygotes (fln/fln) that often failed to thrive to adulthood, development and survival of the heterozygotes (+/fln) showed no apparent difference from their wt (+/+) littermates. However, the +/fln mice developed a progressive degeneration of small sensory fibers, that were observed both behaviorally and functionally. Interestingly, the +/fln showed no obvious structural alterations in their brain and neuronal populations that included NGF-dependent basal forebrain cholinergic neurons (BFCNs). The +/fln mice did not develop appreciable deficits in learning and memory. Our results are in line with data from limited human studies of NGF^{R100W} carriers (Minde et al., 2009, 2004; Minde, 2006). Mechanistically, we showed the R100W mutation resulted in reduced secretion of mature NGF in primary mouse embryonic fibroblasts (MEFs) cultured from our mutant mice. These results are consistent with previous findings(Larsson et al., 2009; Testa et al., 2019b). We believe these in vivo findings will help to reignite efforts of using NGF as a therapeutic agent, that will lead to the development of

'painless NGF' therapies (Capsoni et al., 2011; Cattaneo and Capsoni, 2019; Sung et al., 2019; Testa et al., 2019b).

2. Materials and methods

2.1. Ethical statement

All experiments involving the use of laboratory animals have been approved by the Institutional Animal Care and Use Committee of University of California San Diego. Surgical and animal procedures were carried out strictly following the NIH Guide for the Care and Use of Laboratory Animals. In most experiments, both male and female mice were used. When possible, we made every effort in our experiments to measure differences between male and female animals. Mice that were visibly sick, had wounds or showed any abnormal behaviors such as extreme aggressive behaviors were excluded from all experiments.

2.2. NGF^{R100W} knockin mouse model

NGF^{R100W} knockin mice were generated by the Model Animal Research Center of Nanjing University (Nanjing, Jiangsu, China) as described previously (Yang et al., 2018). Briefly, the arginine (R) at position 100 of mature mouse NGF was mutated to tryptophan (W) by gene targeting (Yang et al., 2018). The Neo cassette has been deleted from the mutant allele. Genotyping identification of NGF^{R100W} knockin mice was carried out by PCR using the primer pairs that recognize sequences near the loxP sites: 5-GGGGAAGGAGGGAAGACATA-3 for forward primer and 5-GATTCCCTTAGGAAGGTTCTGG-3 for reverse primer. The following amplification protocol (95 °C 5 min; 95 °C 30 s; 58 °C 30 s; 72 °C 45 s; 35 cycles; 72 °C 5 min; 15 °C hold) was used for genotyping; the expected PCR products were marked for +/+, +/fln or fln/fln.

2.2.1. Animal housing conditions

All mice were housed in individual cages on a 12/12 h light/dark cycle at 21 ± 2 °C. All animals were provided with free access to water and foods containing no ad libitum. The colonies were regularly monitored by trained staff at UCSD vivarium. All tests were carried out in a quiet room between 10 AM and 4 PM using sex- and age-matched mice.

2.3. Behavioral tests

2.3.1. Nociceptive hot plate test

In nociceptive hot plate test, mice were placed on a metal hot plate at 55 °C (Analgesia Hotplate, Columbus Instruments, Columbus, OH). The latency time to a discomfort reaction (jumping, licking or shaking hind paws) was recorded and the mice were immediately removed from the hot plate and were returned to their home cages. The cut-off time was 20 s.

2.3.2. Morris water maze

The Morris water maze was used to evaluate spatial learning and memory as previously described (Spencer et al., 2017). A platform was placed in the center of one quadrant of the pool (diameter 180 cm). The pool was filled with opaque water (24 °C) until the platform was submerged 1 cm beneath the water surface. Mice were first trained to find a platform with a visible flag on days 1 to 3 and then a submerged hidden platform on days 4–7. Each mouse was placed into the water facing the wall of the pool at its designated departure point. The departure point was changed randomly between two alternative entry points. These points were located at each intersecting line between two zones with the same distance from the platform. Each mouse was trained for four consecutive 90 s trials with a brief rest. Mice that failed to reach the platform within 90 s were held by the tail and guided to the platform and stayed on it for another 30 s. On Day 8 of the probing test, the platform was taken away and mice were let to search the pool for the first 40 s trial. The times spent by mice in the target quadrant and the number of passing of the target zone were recorded. For the second 40 s trial, the visible platform was placed to the same position and the time to find the platform (latency time) by the test mice was recorded.

2.3.3. Y-Maze spontaneous alternation test

The Y-Maze spontaneous alternation test was performed to measure changes in the natural propensity of mice to explore new environments and spatial memory. The test was carried out in a Y-shaped maze with three enclosed black, opaque plastic arms (A, B, C, and 29 cm × 68 cm × 619 cm each) at a 120° angle from each other. Mice were placed into the center of the maze and allowed to freely explore the three arms for 5 min. An entry occurred and was recorded when the hind paws of mice were within the arm. The total number of arm entries and the entering sequence were recorded. A spontaneous alternation performance (SAP) occurred when mice entered three successive different arms (e.g. ABC, BCA, CAB, BAC, ACB, CBA). The SAP percentage was calculated with the following formula: [Total number of SAP/(total arm entries–2)] ×100(Carpenter et al., 2012).

2.3.4. Novel object recognition test

A novel object recognition test was performed with a black open-filed chamber (31 × 24 × 20 cm; length: width: height) to assess short-term and long-term memory impairment in mice (Lueptow, 2017). We used three objects that differred in shape and texture: 1): Lego bricks (L:W:H, 4:2:8 cm) 2:Thermo cell culture polystyrene flasks filled with sand (75 mL) and 3) glass Erlenmeyer flasks filled with sand (50 mL). Object preference was examined in prior experiments with mice of similar age, and mice have equal preferences for those three objectives (Kleschevnikov et al., 2017). On Day 1, mice were habituated in the chamber for 10 min and were returned to their home cage. On Day 2, two identical objects (Lego bricks) were placed in the chamber, and the test mouse was placed to the chamber and allowed to explore both objects for 8 min. After the familiarization, it was returned to the home cage. For the short-term memory impairment test, after 30 min interval, one of the familiar Lego bricks used for memory acquisition was replaced together with a new object (cell culture polystyrene flask filled with sand). The mouse was placed in the chamber for 8 min to explore the objects. On day three, for the long-term memory impairment test, after 24 h interval, one of the Lego bricks was replaced with another new object (glass Erlenmeyer flask filled with sand). The test mouse was allowed to explore the objects for 8 min. The activities of mice during the test were recorded with a video camera and the time spent exploring each object was quantitated. The discrimination ratio was calculated with the following formula: discrimination ratio (%) = time spent exploring novel object/total time spent exploring both objects) ×100.

2.3.5. Marble burying test

The marble-burying test was performed to evaluate the anxiety-like behavior in mice (Thomas et al., 2009). Twenty marbles were equidistantly placed (5 × 4) on the bedding surface (see Fig S4). After 20 min, the number of marbles buried (> 50 % of its surface area is covered by bedding) was counted.

2.3.6. Light-dark shuttle box test

The light-dark shuttle box test was carried out to evaluate the anxiety-like behavior in mice as well (Heredia et al., 2014). The apparatus consists (21 × 42 × 25 cm, L:W:H) of two equally sized chambers, a black chamber and a brightly illuminated white chamber that were connected through a door. The test mouse was placed in the dark chamber facing away from the opening of the door for 3 s before the door was open. Mice were allowed to move freely between the two chambers for 10 min. The latency to first cross to the light chamber from the dark chamber and the time spent in the bright chamber were recorded.

2.3.7. Social interaction test

Social interaction test was performed to measure the social memory impairment in mice (Kaidanovich-Beilin et al., 2011). The apparatus (40.5cm × 60cm × 22 cm) consists of three equally sized chambers connected by doors. Two wire containment cups (a height of 15 cm and diameter of 7 cm) are placed in the two side chambers respectively. Prior to the test, the doors were closed and the two test mice were placed at the center of the middle chamber for 5 min to familiar with its surroundings. After the habituation, for the social affiliation aspect of the test (session I), one of the control mice (Stranger 1) was placed inside one of the two cups that were located in one of the side-chamber. Another cup was empty. The test mouse was placed to the middle chamber and the doors were opened. The mouse was allowed free access to the subject mouse to explore each of the three chambers for 10 min. For social novelty/preference session of the test (session II), the control mouse (Stranger 2) was placed to the empty cup in the opposite side chamber. Same parameters as in session I were recorded for another 10 min. The duration of contacts between the test mouse and the empty cup or Stranger 1 in session I, or between the test mouse and Stranger 1 or Stranger 2 in session II were recorded.

2.4. Chemicals, antibodies

Unless specified, all chemicals were purchased from either Sigma or Fisher. Mouse hindpaw skin sections were stained with the UCHL1/PGP9.5 rabbit polyclonal antibody (Cat.No. 14,730-1-AP, Proteintech Group, Inc, Rosemont, IL) at a dilution of 1/300 to 1/500. DRG sections were stained for CGRP using a rabbit antibody (Cat.No 19005, OWL), or a mouse antibody (Cat. No 57053, Santa Cruz Technology) at a dilution of 1/300. A rabbit anti-TrkA antibody (RTA, a generous gift from Dr. L. Reichardt) or a rabbit anti-TrkB antibody (BiossUSA, Cat# bs-0175R-FR) was also used to stain DRG sections. Brain sections were stained with a mouse anti NeuN antibody (Cat.No MAB377B, Millipor1e, Billerica, MA, USA) at a dilution of 1/100. Biotinylated horse anti-mouse IgG antibody (Cat.No. BA2000, VECTOR LABORATORIES, INC. Burlingame, CA) was used at a dilution of 1;100. Biotin-conjugated donkey anti-rabbit IgG (Cat. No 711-065-152, Jackson ImmunoResearch, West Grove, PA, USA) was used at with dilution of 1;100. Goat secondary anti rabbit or anti mouse IgGs conjugated to Alexa 488 or Alexa 568 (ThermoFisher) were used at 1/800 dilution.

2.5. Immunohistochemistry

2.5.1. Histomorphometric analysis of the sciatic nerve

Mice were anesthetized using isoflurane and sacrificed with a guillotine. Sciatic nerves were collected and fixed in 2.5 % glutaraldehyde (in 0.1 M sodium phosphate buffer) for 24 h at 4°C. Nerves were then rinsed with 0.1 M sodium phosphate buffer and postfixed in 2 % osmium tetroxide (1 mL 4 % osmium tetroxide + 1 mL 0.2 M sodium phosphate buffer) for 30 min at room temperature. Nerves were rinsed with distilled water twice and then dehydrated through graded ethanol (10 min each in 30 %, 50 %, 70 %, twice in 95.5 % for 15 min for each rinse, and twice in 100 % for 15 min for each rinse). Samples were then rinsed in propylene oxide twice for 15 min for each rinse and then put in a mixture of 50 % propylene oxide and 50 % resin for at least 2 h. Finally, samples were embedded in 100 % resin and sectioned using a glass knife and microtome to 0.5 μm semi-thin section. Sections were stained with 2 % P-Phenylene Diamine (PPD) at room temperature for approximately 20 min and analyzed with a light microscope. The diameter of myelinated fibers was measured using NIH ImageJ.

2.5.2. Staining of dorsal root ganglion (DRG) and brain sections

L3-L5 DRGs were collected and fixed in 4 % paraformaldehyde for 30 min at 4 °C, and then permeated with 15 % sucrose at 4 °C overnight. DRGs were then embedded in Tissue-Tek O.C.T (Electron Microscopy Sciences, Hatfield, PA) and sectioned into 20 μm cryo-sections. Brains were dissected and fixed in 4% paraformaldehyde for 5 days at 4 °C. Brains were then sectioned using vibratome to 40 μm. Sections were incubated in 1 % Triton X, 10 % H_2O_2 in PBS for 20 min at room temperature, washed three times with PBS, blocked 1 h at room temperature with 10 % goat serum and then incubated with primary antibodies overnight. Sections were then incubated with biotinylated secondary antibody at 1:100 made in PBS for 30 min at room temperature, washed with PBS three times, incubated with avidin-biotin-peroxidase (ABC Kit, VECTOR LABORATORIES, INC. Burlingame, CA) for 1 h and followed by peroxidase detection (DAB Kit, ABC Kit, VECTOR LABORATORIES, INC. Burlingame, CA). Finally, sections were mounted and analyzed with a light microscope (Leica DMi8 Live Imaging Microscope).

2.5.3. Staining of hind paw footpad skin

Skin samples were dissected and fixed in methanol/acetone (1:1) for 30 min at −20 °C, rinsed with PBS three times, and incubated in 30 % sucrose overnight at 4 °C. Tissues were embedded in Tissue-Tek O.C.T (Electron Microscopy Sciences, Hatfield, PA) and sectioned into 45 μm cryo-sections using a Leica Cryostat (Model# CM1900). Sections were incubated in 50 mM Glycine for 45 min at room temperature, rinsed in PBS three times, blocked in 10 % goat serum, 1 % BSA, 0.5 % Triton X in PBS and then incubated with primary antibodies overnight at 4 °C. Primary antibodies were diluted in 10 % goat serum, 1 % BSA, 0.2 % Triton X in PBS. Sections were rinsed three times with PBS and then incubated with secondary antibodies at room temperature for 1 h. After washing with PBS three times, sections were mounted and analyzed by confocal microscopy (Leica TCS SP8 Confocal Microscope). Approximately, for samples from each animal, we examined 10–15 sections with 200 μm in length/section. The image stacks were collected at a 0.5 μm step size. Maximal projection images were generated from these stacks and the IENF density was quantified using ImageJ.

2.6. Primary culture of mouse embryonic fibroblasts and ELISA measurement of NGF

Skin samples were dissected from mouse E16−18 (+/+, +/fln and fln/fln) embryos. Following dissociation, fibroblasts were cultured in 6 well plate in DMEM supplemented with 4.5 g glucose, 10 % FBS and 1 % penicillin/streptomycin. At 70–80 % confluency, the cultures were changed to serum-free medium for 48 h. Media were collected and NGF secreted into media was measured by commercial ELISA (Cat. No. OKBB00230, Aviva Systems Biology, San Diego, CA), following manufacture's protocol.

2.7. Statistical analysis

Statistical analyses were all carried out using GraphPad Prism (GraphPad Software, Inc, La Jolla, CA). For two group comparisons, Student's *t*-test was performed. For multiple comparisons, one-way ANOVA or Two-way ANOVA was performed. All data were represented as mean values ± SEM. $P < 0.05$ was considered statistically significant differences.

3. Results

3.1. The NGF^{R100W} knockin mouse model

To better investigate the impact of NGF^{R100W} mutation, we and other investigators have generated knockin mouse models (Testa et al., 2019a, b; Yang et al., 2018). Testa and colleagues introduced a human NGF allele harboring the R100W mutation to replace mouse endogenous NGF allele (Testa et al., 2019a, b). We simply generated a knockin mouse model of HSAN-V NGF^{R100W} that carried the mouse NGF allele (Yang et al., 2018). Herein, we will refer the wildtype mice as +/+, the heterozygous mutant mice as +/fln, the homozygous mutant

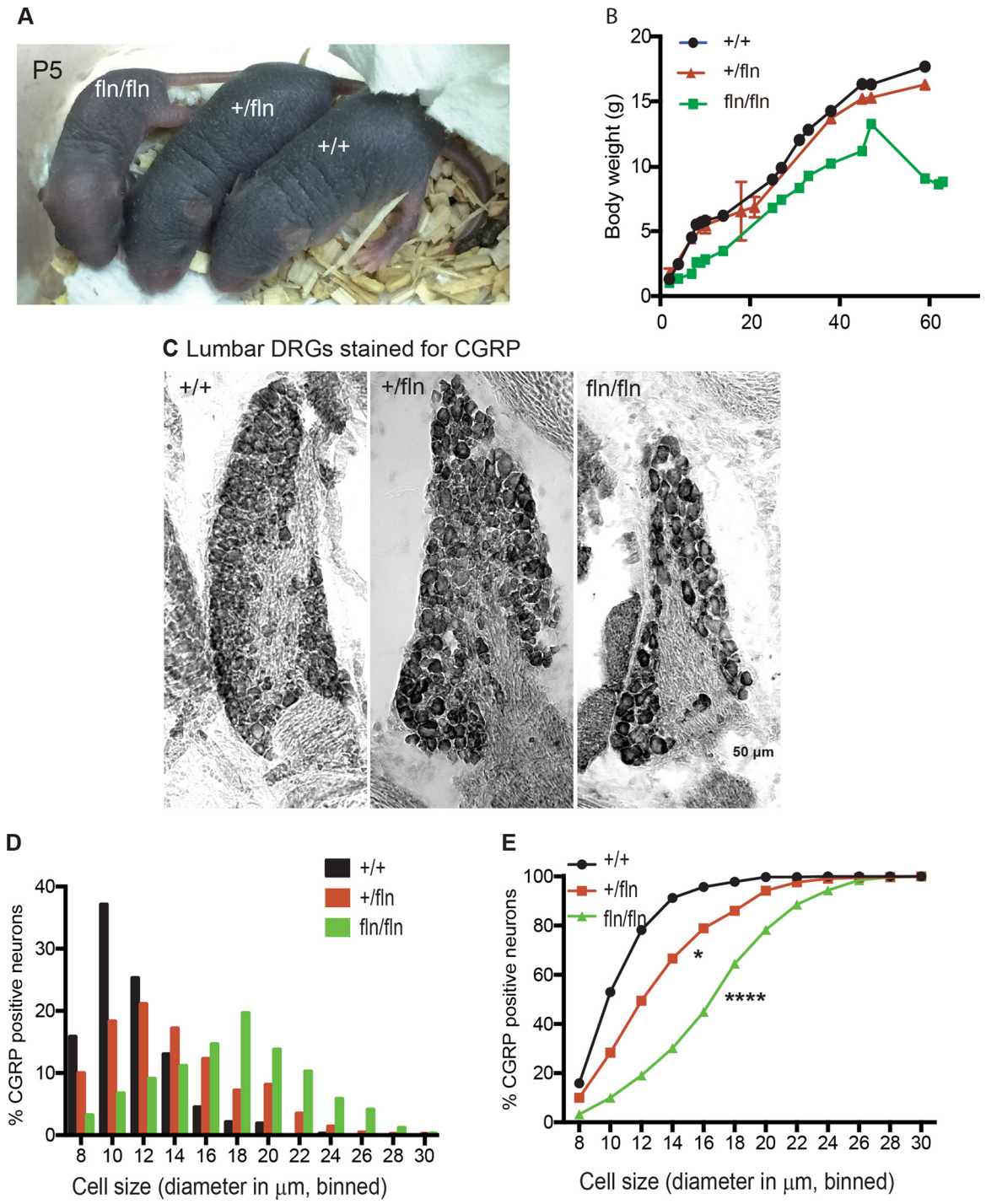

Fig. 1. The +/fln and fln/fln mutant mice exhibit loss of CGRP-positive neurons in DRGs. (A) The body weight of three genotype was monitored over a period of 8 weeks (+/+: n = 3; +/fln: n = 5; fln/fln: n = 3). (B) Pups of the three genotypes at postnatal 5 days. (C) Immunoreactivity to CGRP in representative sections of lumbar DRG from P0 mice. (D) Cell size distribution of CGRP-positive neurons in DRG. +/+: n = 3 (423 cells); +/fln n = 3 (431cells); fln/fln: n = 3 (341 cells). All p values were calculated using nonparametric Kolmogorov-Smirnov test. (E) Cumulative distribution of CGRP-positive neurons in DRG. *=p < 0.05, ****=p < 0.0001, one-way ANOVA test followed by Dunn's multiple comparisons test (compared with +/+ group).

mice as fln/fln. Representative pictures of pups at P5 of the three genotypes are shown in Fig. 1A. Our observations during the early postnatal days showed that the fln/fln mice displayed smaller milk spot in the stomach and often died within the first week of life. Through reducing the litter size by moving littermates with bigger milk spot (presumably +/+) at P1 to a surrogate mother, we were able to rescue some of the fln/fln mice. Some of these mutant mice could ingest more milk and survived up to 6 weeks to 2 months. The fln/fln mice were born with normal body weight but gained weight more slowly after birth with 75 % of the mean weights of their wild type mice at 4 weeks of age (Fig. 1B). The fln/fln mice also showed developmental delay in many other aspects, including eye opening and hair growth. The heterozygous mice (+/fln), on the other hand, exhibited normal body weight and could not be distinguished from their littermates by their appearance and spontaneous behaviors (Fig. 1A, B).

3.2. The fln/fln mice exhibits severe loss of PGP9.5-positive intra-epidermal sensory fibers (IENFs) and CGRP-positive small sized neurons in dorsal root ganglia (DRG)

We previously analyzed and quantitated the density of intra-epidermal sensory fibers (IENFs) by staining for PGP9.5 in the hind paw skins from postnatal 0 (P0) day mice of all three genotypes(Yang et al., 2018). We demonstrated the fln/fln pups, but not the fln/+ mice, show a significant decrease in IENF density in comparison with the +/+ mice (Yang et al., 2018).

DRG neurons convey sensory information from the periphery to the CNS (Meyer et al., 2006; Willis, 2004). Pain sensation is primarily conveyed by small DRG neurons (≤ 30 um)(Li et al., 2016; Meyer et al., 2006; Willis, 2004), which are predominantly marked by the calcitonin gene-related peptide (CGRP) (Li et al., 2016). To investigate if this population of DRG neurons were affected by the R100W mutation, we extracted lumbar DRGs from +/+, +/fln and fln/fln P0 pups. DRGs were processed and stained with a specific antibody against CGRP. Representative images of the three genotypes are presented in Fig. 1C. Strikingly, the CGRP-positive neurons in the fln/fln samples showed a significant reduction in the small size neurons (Fig. 1C, E). The soma sizes of CGRP-positive neurons were quantified and the size distributions for each genotype are shown in histograms and cumulative percentage plot (Fig. 1D and E). The majority of CGRP-positive neurons (−90 %) in the +/+ samples fell within the range of 8−14 μm in diameter. DRGs from the +/fln samples exhibited a size distribution pattern similar to +/+, although with a slight increase in the range of 18−22 μm (Fig. 1 D and E). The fln/fln sample showed a marked decrease in small size neurons (8−14 μm) (−35 % versus −90 % in +/+) (Fig. 1 D and E). The large size neurons (≥16 μm) in fln/fln was increased to −65 % as compared to −10 % in the +/+ DRGs. These observations become more evident in the cumulative percentage plot that was significantly shifted to the right in fln/fln as compared with +/+. Taken together, these data have demonstrated that the NGF^{R100W} mutant allele, especially presented in two copies, results in a marked reduction in the number of both IENFs in the skin and CGRP-positive small size neurons in DRGs.

3.3. The fln/fln mutant mice show severe deficits in sensing hot temperature

Given that both IENFs and small size DRG neurons were severely reduced in the fln/fln mutant mice, we predicted that these mice would develop severe deficts in perceiving painful stimuli. We next used a hot plate assay (55 ˚C) to test the threshold of 2 month-old mice to thermal stimuli using a 20 s cutoff. As showed in Fig. 2A, there was no significant difference between the +/+ and +/fln mice, both with an average latency time of −11 s. However, the latency time for the fln/fln mice was significantly increased. The fln/fln mice were totally insenitive to the 55 ˚C thermal stimuli and showed no signs of discomfort on the hot plate. In the end, they had to be immediately removed at the 20 s cutoff. Together with the observation of severe reduction of both IENFs and small-size DRG neurons in the fln/fln P0 pups, these results provide strong evidence that the fln/fln mice have lost their ability to perceive and respond to noxious stimuli, a telltale sign for severe peripheral sensory neuropathy. Therefore, the NGF^{R100W} knockin mouse model recapitulates one of the most prominent clincial manifestations of peripheral sensory neuropathy in HSAN V patients (Einarsdottir et al., 2004; Minde et al., 2009, 2006; Minde et al., 2004; Minde, 2006).

3.4. The +/fln mice show progressive loss of small size CGRP-positive neurons in DRGs

Although HSAN V is classified as an autosomal recessive disease (Einarsdottir et al., 2004), heterozygous patients have been also shown to develop sensory neuropathy albeit to a lesser severity with an adult onset (Minde et al., 2009, 2004; Perini et al., 2016; Sagafos et al., 2016). Since the fln/fln mice often failed to survive to adulthood in sufficient numbers for performing experiments, we decided to focus our effort on the +/fln mice herein.

We measured the density of CGRP- and TrkA-positive neurons in DRGs in the +/fln mice at different ages (4- and 10-months) and compared with their littermate +/+ controls. Representative images (CGRP, TrkA and merged images) along with qunatitative results are shown in Fig. 3A and B. The +/fln mice at 4 months of age did not show a differenece from their same age +/+ littermates with regarding the number of either CGRP-positive, or TrkA-positive or CGRP/TrkA-double positive neurons (Fig. 3A and B). However, these vaules showed a marked change at 10 months in the +/fln mice compared to the +/+ mice: the percentile of small size CGRP-positive and CGRP/TrkA-positive neurons were significantly reduced, while the percentile of TrkA-positive DRG neurons was not significantly affected (Fig. 3A and B).

To investigate if there was also a decrease in large-diameter DRG neurons in the +/fln mice, we performed additional analysis for TrkB-positive neurons in DRGs. TrkB has been shown to be co-expressed in with NF200 primarily in large diameter DRG neurons as demonstrated by unbiased single cell sequencing of mouse DRGs (Usoskin et al., 2015). Following the same protocol as outline above, we stained DRG sections with a specific antibody against TrkB and a specific antibody against CGRP (Fig. 4A). Our quantitative results showed that the number of TrkB-positive DRG neurons in 10 month-old +/fln mice showed no significant changed as compared to the age-matched +/+ mice (Fig. 4B). Consistent with Fig. 3, the number of CGRP-positive neurons was decreased in the +/fln samples. Taken together, our results are evidence that small diameter DRG neurons are selectively decreased in the +/fln mice.

We next examined if myelinated fibers were affected in the +/fln mice. We extracted sciatic nerve and stained myelinated fibers with p-phenylene diamine (PPD) at different ages (2-, 9- and 18-months). Our results have revealed that the median values of myelinated fiber

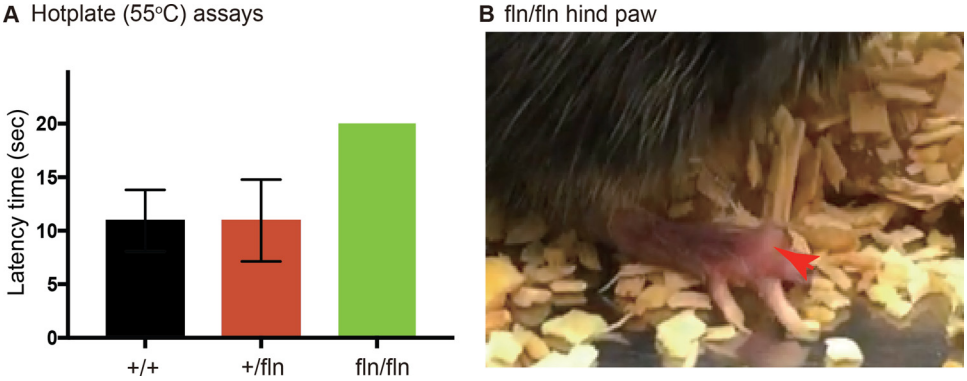

Fig. 2. The fln/fln mutant mice display decreased responsiveness to pain at 2 months of age. (A) The fln/fln, not +/fln mutant mice showed significant deficits (20 s, cutoff time) in 55 ˚C hot plate assays at 2 months of age. Mean ± SEM, * = $p < 0.05$, ** = $p < 0.01$ by unpaired t test. +/+: n = 39; +/fln: n = 29; fln/fln: n = 2. (B) The fln/fln mutant mice showed serious hind paw damage after hot plate test.

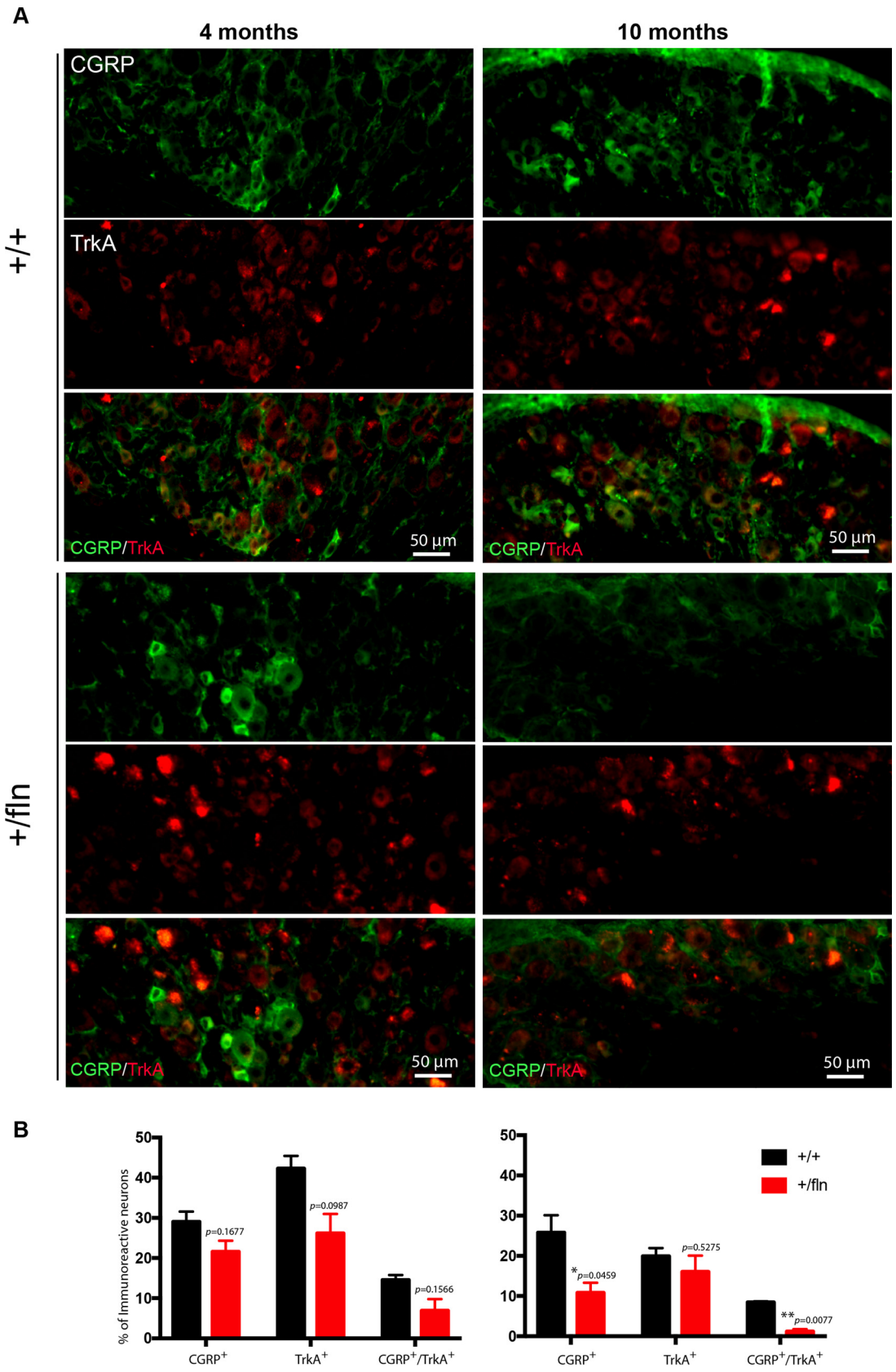

Fig. 3. The +/fln mice exhibit progressive loss of CGRP/TrkA-positive small sized DRG neurons. A: Images of representative sections of lumbar DRGs stained for CGRP/TrkA in +/+ and +/fln mice at 4 and 10 months of age. B: The quantitative results are shown. 3 pairs of mice (n = 3) were examined in each condition. The data were analyzed by t test.

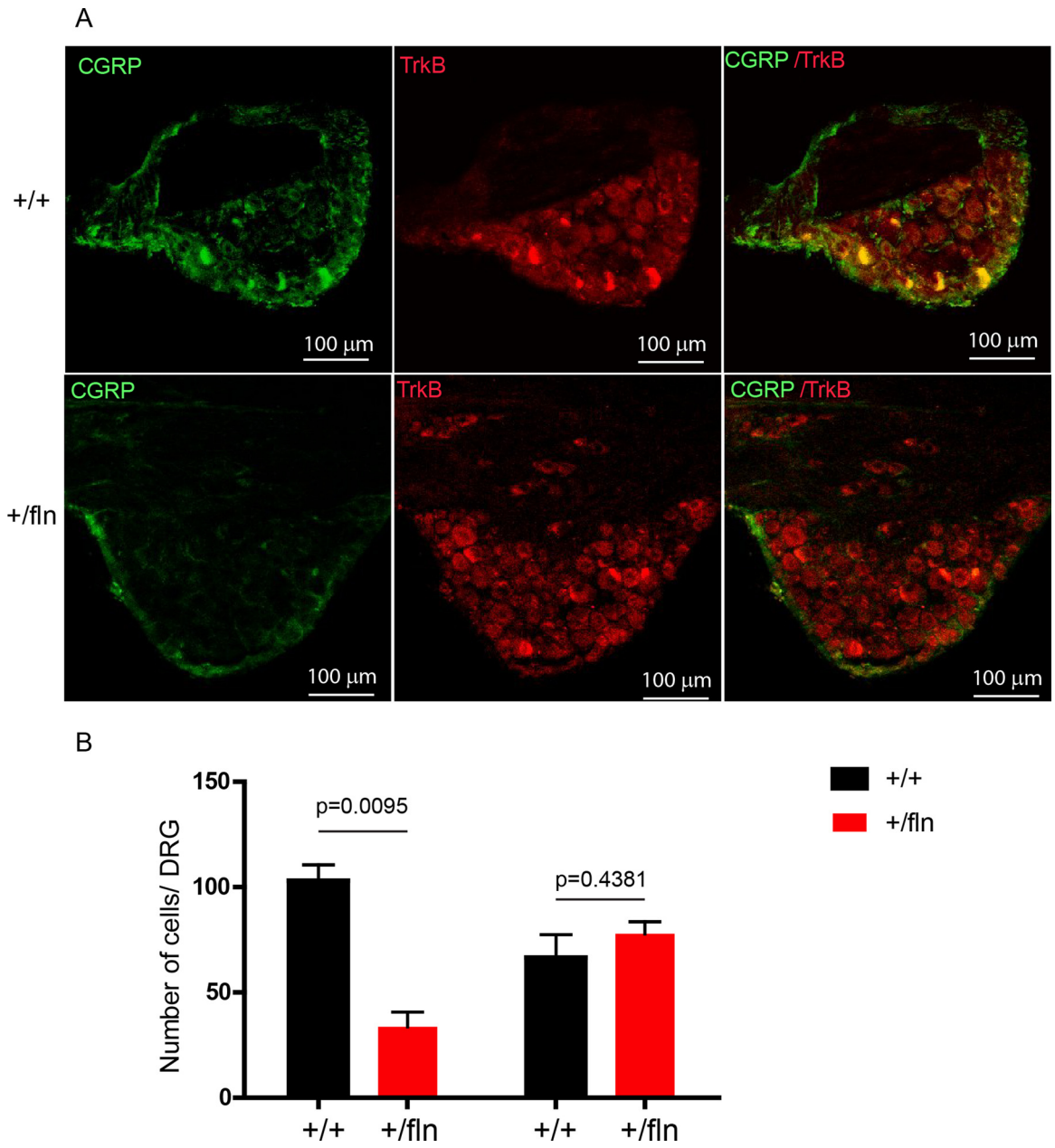

Fig. 4. The +/fln mice exhibit no loss of TrkB-positive large diameter DRG neurons. A: Images of representative sections of lumbar DRGs stained for CGRP/TrkB in +/+ and +/fln mice at 10 months of age; B: The quantitative results. 3 pairs of mice (n = 3) were examined in each conditions. The data were analyzed by t test.

diameters in both +/+ and +/+ mice at 2-, 9- and 18 months of age were between 6 and 12 μm (Fig. 5 A–C). Statistical analysis showed non-significant difference between the two genotypes in size distribution of myelinated fibers. Taken together, these results have demonstrated that a single NGF^{R100W} mutant allele results in a progressive loss of CGRP-positive small sized sensory neurons in DRGs with no apparent loss or shrinkage of myelinated fibers in their sciatic nerve.

3.5. The +/fln mutant mice exhibit progressive degeneration of PGP9.5-positive IENFs

At P0, the fln/fln mice but not the +/fln mice, showed significant reduction in the density of IENFs in the skin as compared to their +/+ littermates (Yang et al., 2018). The difference among the three genotypes can be best visualized by the reconstituted 3-D images of IENFs in the hindpaw skins of +/+. +/fln and fln/fln (Movie S1, S2 and S3, respectively). More importantly, the +/fln mice showed no sensory deficits in hot plate assays at 2 months of age (Fig. 2), suggesting that they developed normally to adulthood. To investigate if the +/fln mice developed progressive sensory neuropathy, as observed in HSAN V heterozygous patients (Einarsdottir et al., 2004), we next measured the density of IENFs in both +/fln and +/+ mice at different ages (2, 9, 18 months). Using the same methods (Yang et al., 2018), we quantified the density of IENFs in the hind paw skin. Representative images of skin sections stained with anti-PGP9.5 antibodies (Fig. 6A). Our results have revealed that the +/fln mice indeed showed a progressive loss of IENFs. Quantitative analysis showed no signifciant differences between the +/fln and +/+ mice at 2 months of age (Fig. 6B). At 9 months of age, the +/fln mice showed a marked reduction in the IENF density (Fig. 6A, B). At 18 months of age, IENFs were hardly detected in the +/fln mice (Fig. 6A and B, Movie S4 and S5). Taken together, these results have demonstrated that a single NGF^{R100W} mutant allele results in a progressive degenerative phenotype of small sensory fibers.

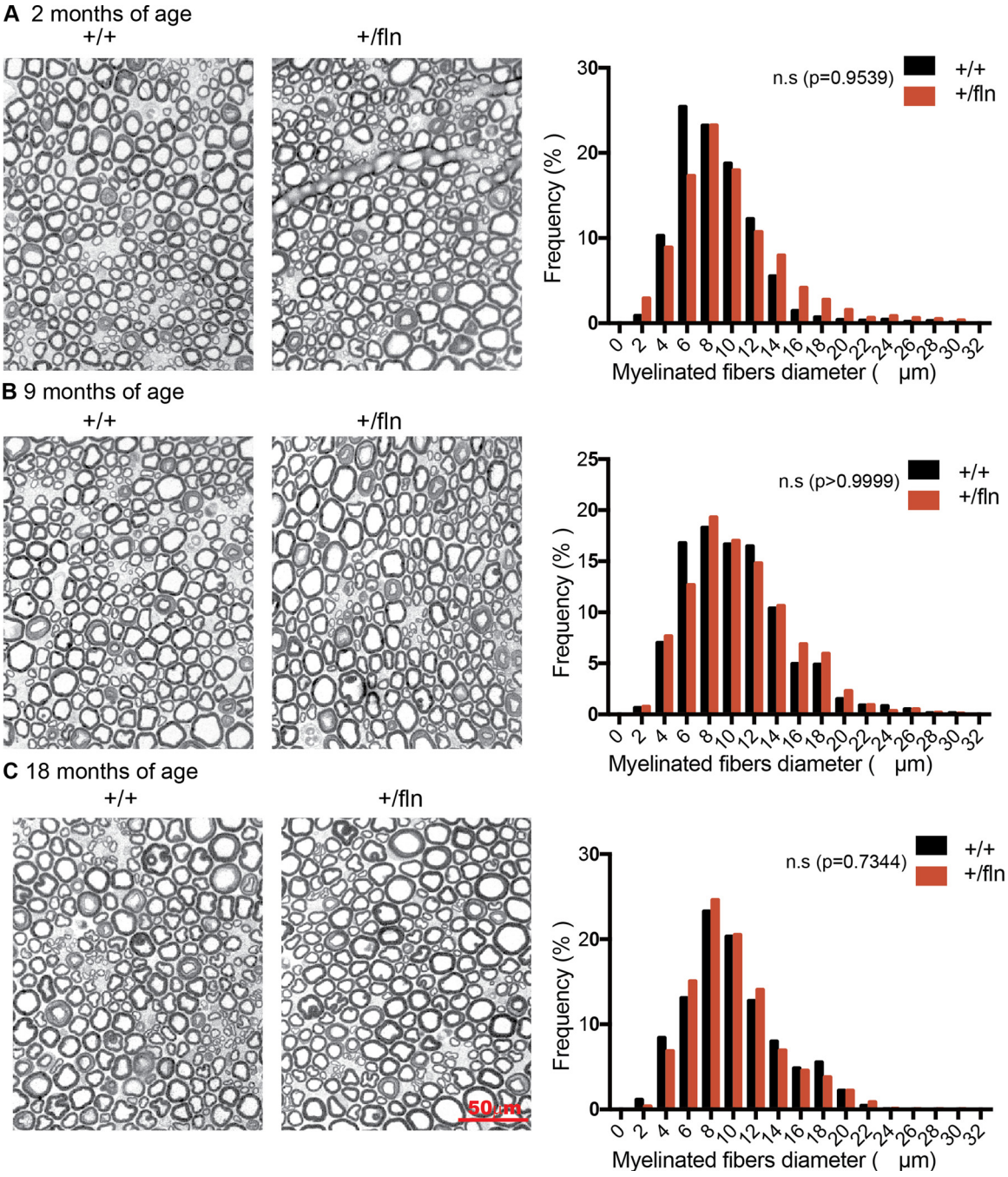

Fig. 5. The +/fln mice show no loss of myelinated fibers in sciatic nerve by *P*-Phenylene Diamine (PPD) staining. (A), (B), (C) Representative sections of the myelinated fibers in sciatic nerve from +/+ and +/fln mice of 2, 9 and 18 months of age respectively. Side panel was the size distribution of the myelinated fibers. One pair mice per group, 2 month (+/+, n = 2718 fibers; +/fln: n = 3682 fibers), 9 month (+/+: n = 1685 fibers; +/fln: n = 3524 fibers), 18 month (+/+: n = 1661 fibers; +/fln: n = 806 fibers). All p values were calculated using nonparametric Kolmogorov-Smirnov test.

3.6. The +/fln mutant mice develop progressive nociceptive deficits

Given that the +/fln mice showed progressive structural degeneration: reduction in both the numbers of IENFs and small sensory DRG neurons, we predicted that these mice would develop nociceptive deficits. We again used the hot plate assay to assess the pain sensitivity of the +/fln mice of 2-, 9- and 18-months of age in comparison with their respective +/+ littermate controls. Consistent with the results from studies of IENFs and DRGs, our results demonstrate that the +/fln mice began to show deficits in nociception at 9 months of age with the deficits becoming more pronounced at 18 month (Fig. 6 C). These results indicate that the +/fln mice develop progressive nociceptive deficits.

3.7. The +/fln mice exhibit no marked structural changes in the brain

The impact of NGF^{R100W} mutation on progressive degeneration of the PNS both structurally and functionally raised the question if the CNS was also affected in our mouse model of HSAN V. NGF is mainly produced in the hippocampus and retrogradely transported to the basal forebrain to support survival and differentiation of BFCNs (Mobley et al., 1986; Pezet and McMahon, 2006). To address this, we examined the brain sections from 12-month-old +/fln and +/+ mice. Neurons were identified by immunostaining the sections with a specific antibody

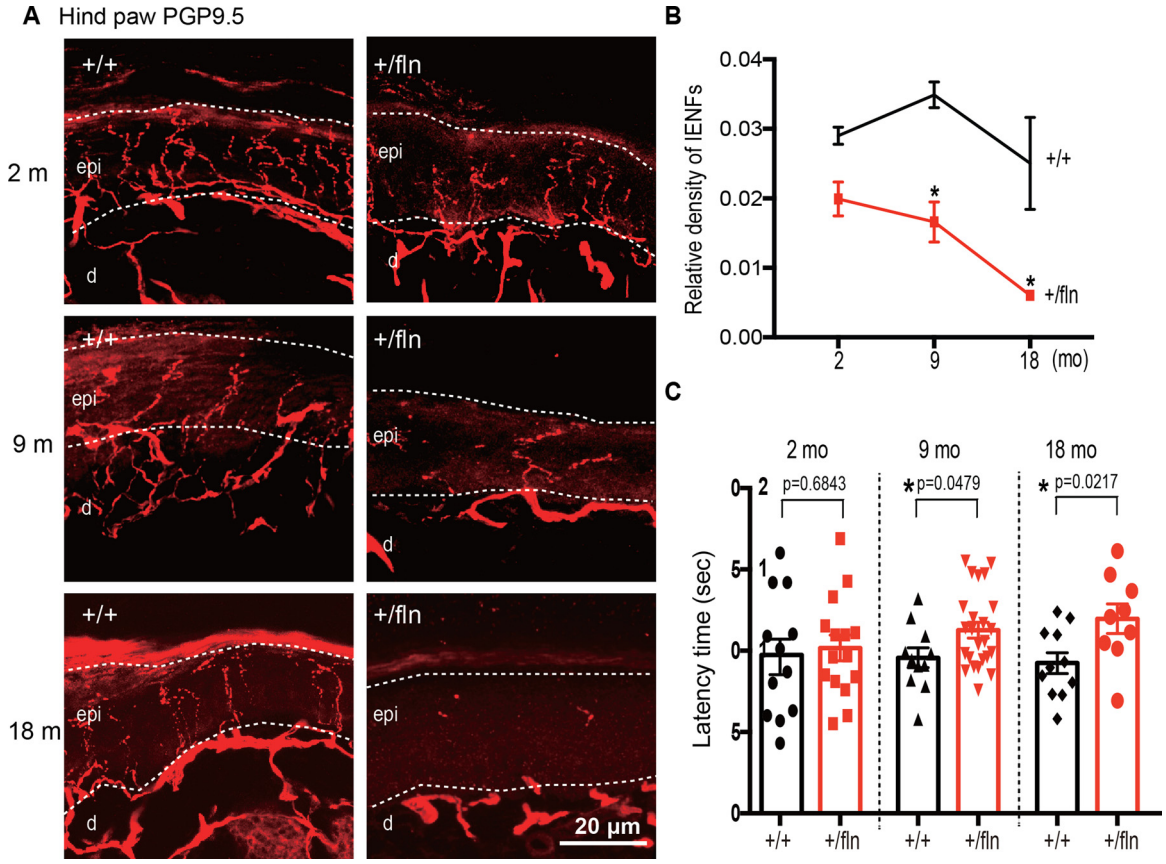

Fig. 6. The +/fln mutant mice exhibit progressive loss of PGP9.5-positive intra-epidermal sensory fibers (IENFs) and develop progressive sensory deficits. (A) Sections of footpad skin from 2-, 9- and 18 month-old mice were stained with antibodies to the pan-nerve fiber marker PGP9.5. (B) Quantification of PGP9.5-positive nerve fibers intensities in epidermis of footpad skin. To estimate the density of IENF in the epidermis, at least 12-15 images of each animal were analyzed throughout the section thickness and entire length of each image. About 2600 um of footskin per each animal was analyzed. epi: epidermis ; d: dermis. Mean ± SEM, * = $p < 0.05$ by two-way ANOVA test. +/+: n = 3; +/fln: n = 3; (C) Hot plate assays at 2, 9 and 18 months of age. Mean ± SEM, * = $p < 0.05$ by two-way ANOVA. 2 month-old mice (+/+: n = 12; +/fln: n = 15), 9 month (+/+: n = 11; +/fln: n = 27), 18 month (+/+: n = 11; +/fln: n = 9).

to NeuN, a marker of neurons. We were particularly focused on the hippocampus and basal forebrain. As illustrated in Fig. S1A, NeuN-immunoreactive neurons were densely compacted in the stratum pyramidale of hippocampal CA1 and CA3 regions and in the dentate gyrus (DG) regions in both the +/fln and +/+ brains. We measured the thickness of CA1, which revealed not significant difference between +/+ (34.48 ± 0.65 μm) and +/fln (35.52 ± 1.01 μm) mice hippocampus. (Fig. S1A and C). To determine the impact of NGF^{R100W} on the development of basal forebrain, we analyzed the density of medial septum by quantifying the average NeuN-positive fluorescence intensity in the medial septum. Our results showed that the density of NeuN-immunoreactive neurons was not significantly different between 12-month-old +/+(30,804 ± 2367 A.U./mm^2) and +/fln (33,021 ± 8066 A.U./mm^2) mice (Fig. S1B and C).

In the central nerve system, sensations such as pressure or pinprick are registered in the somatosensory cortex, whereas pain is perceived in anterior cingulate cortex (ACC) where emotional reaction to pain is dealt with concomitantly (Price, 2000). It has been suggested that compared to healthy individuals, NGF^{R100W} carriers seem to show weaker blood-oxygen-level-dependent response in their ACC regions using functional MRI (Morrison et al., 2011). Given that pain perception is significantly reduced in the +/fln mice at the age of 12 months, we investigated if the progressive loss of pain perception involved any central component such as changes in ACC. We quantified NeuN-positive neurons in ACC, as marked by the red dashed box in the sagittal brain section of +/+ and +/fln mice (Fig. S2A). Our data show there was no significant difference in the density of NeuN-positive signals between +/+ (1903 ± 88.96 A.U./mm^2) and +/fln (1689 ± 65.52 A.U./mm^2) (Fig. S2B and C). Taken together, these results have indicated that the +/fln mutant mice show no apparent structural changes in their ACC that could also contribute to loss of pain perception.

3.8. The +/fln mice show no apparent deficits in CNS dysfunction

One of the major clinical features that distinguish the NGF^{R100W}-associated HSAN V patients from HSAN IV associated with mutations in TrkA is that HSAN V patients do not suffer from overt cognitive deficits (Capsoni, 2014; de Andrade et al., 2008; Einarsdottir et al., 2004; Haga et al., 2015; Minde et al., 2004). To test if this is the case in our HSAN V mouse model, we performed a battery of behavioral tests to assess cognitive functions.

The Y-Maze spontaneous alternation test was performed to evaluate the working memory (Carpenter et al., 2012). Mice prefer to enter a new arm of the maze rather than return to one that was previously explored. As illustrated in Fig. S3A, there were no significant differences in the number of arm entries or alternation rate between the +/+ and +/fln mice at either 9- or 18 months of age. These results suggest that there was no working memory impairment in the +/fln mice.

We next used a novel object recognition assay to assess short- and long-term memory (Lueptow, 2017). Following acclimating to a designated object (will serve as the familiar object), the test subject was given the familiar object and a novel object at either 30 min or 24 h for measuring short- and long-term memory, respectively. We found that at 9, 18 months of age, the +/fln mice displayed no difference from their

+/+ littermate controls in either short-term memory (Fig. S3B). The +/fln mice at 18 months of age appeared to show a difference from the +/+ in long-term memory in this test.

We then tested these mice for social interactions, which are critical for mice to maintain social hierarchy and make mate choices (Kaidanovich-Beilin et al., 2011). The three-chamber sociability interaction test was performed to measure both the sociability and social novelty. In Session I of this test, a test mouse normally preferred to interact with another mouse over empty cup, the time that this test subject spent with the live mouse is designated sociability. In Session II of the test, the test subject was provided with either the familiar mouse or another novel mouse, the time that the test mouse spent with the novel mouse is designated as social novelty. As shown in Fig. S3C and D, there were no significant differences between the +/fln and +/+ mice at either 9- or 18-months of age. We conclude that the +/fln mice show no apparent impairment in either their sociability or social novelty.

We also used the marble-burying test to investigate whether the +/fln mice displayed anxiety-like behavior at 9 months of age (Thomas et al., 2009). When placed in a cage with marbles, mice exhibit digging behavior and bury the marbles, which is interpreted as anxiety related. As showed in Fig. S4A, although not statistically significant difference, there was a trend that the +/fln mice buried more marbles than the +/+mice. These results suggest that the +/fln mice were likely more anxious. To further confirm this, we next performed dark-light shuttle box test using 9- and 18-month old mice, which is also extensively used to test anxiety-like behavior (Heredia et al., 2014). Typically, mice show natural spontaneous exploratory behaviors when placed in a new environment and an innate aversion to brightly illuminated areas. When the test subject was placed in the dark-light shuttle box, its exploratory activity will reflect the balance between those two tendencies and will be influenced by the level of anxiety. Decreased time spent in the light chamber has been used as an index of anxiety. Our results showed that the +/fln mice at 9 and 18-months of age displayed no significant difference from age-matched littermate +/+ controls in terms of either the time exiting the dark-chamber or the time spent in the light chamber (Fig. S4B). These results suggest that the +/fln mice likely show no anxiety-like behavior.

To test if the +/fln mice at 18 month showed any deficit in their executive function, we used the Morris water maze (Fig. 7A) to evaluate spatial learning and memory (Spencer et al., 2017). Test mice were first trained to find a platform with a visible flag on Day 1–3 and then a submerged hidden platform on Day 4–7. The path length and time to find the platform (latency time) was recorded. Our result showed the +/fln mice did not differ significantly from the +/+ mice in training curve (Fig. 7B-C). On Day 8 of the probe test, for the first 40 s trial (session I) with the removal of the platform, mice were let to search in pool. We recorded both the time that mice spent in the target quadrant and the number that mice passed the target zone. Our results showed no difference in either measurements (Fig. 7D, E) between the +/fln and age-matched littermate +/+ controls. In the second 40 s trial (session II), the visible platform was re-installed and the latency time was recorded. Again, our test results revealed no significant difference in the latencies between the +/fln and +/+ mice (Fig. 7F).

Taken together, consistent with clinical findings of HSAN V patients (Capsoni, 2014) and with the mouse model examined by Testa and colleagues (Testa et al., 2019a, b), our results have demonstrated that the +/fln mice develop no marked deficits in their CNS dysfunction while exhibiting progressive peripheral degeneration both structurally and functionally.

3.9. NGF^{R100W} mutation results in reduction in NGF secretion

To investigate if reduced secretion in NGF could account for the degeneration of peripheral sensory structures and functions, we explored the possibility that R100W mutation impaired the secretion of mature NGF as suggested previously (Carvalho et al., 2011; Larsson et al., 2009; Testa et al., 2019b). We dissected and cultured primary mouse embryonic fibroblasts (MEFs) of from E18 embryos of +/+, +/fln and f;n/fln. Media were collected and the levels of secreted NGF were measured using an ELISA kit. Our data have revealed that MEFs from either the fln/fln (88.32 ± 6.11 pg/mL) or +/fln (92.49 ± 11.60 pg/mL) mice secreted significantly less amount of NGF as compared to MEFs from the +/+ mice (172 ± 22.06 pg/mL) (Fig. 8). This is consistent with our previously published literature showing a significantly lower yield of NGF^{R100W} recombinant protein from 293FT culturing media (Sung et al., 2018). Therefore, reduced secretion of NGF contributes, at least partially, to the peripheral sensory phenotypes as observed in our mouse model.

4. Discussion

NGF plays a critical role in supporting the survival and differentiation of specific neuronal populations (Chao, 2003; Huang and Reichardt, 2001; Levi-Montalcini, 1987, 2004; Levi-Montalcini et al., 1995; Levi-Montalcini and Hamburger, 1951; Mobley et al., 1986). Since its discovery, NGF has been extensively explored for its therapeutic potential for treating neurodegenerative diseases (Apfel, 2002; Apfel et al., 1998; Eriksdotter Jonhagen et al., 1998; McArthur et al., 2000; Olson, 1993; Quasthoff and Hartung, 2001). However, NGF has also been found to induce severe nociceptive responses (Lewin et al., 1993). The severe side effects of pain-inducing function have largely prevented clinical applications of NGF.

The naturally occurring NGF^{R100W} mutation in HSAN V patients (Minde et al., 2004) offers important insights into two important functions of NGF: trophic and nociceptive actions. HSAN V is caused by a missense mutation in NGF gene (661C > T), which leads to a substitution of tryptophan (W) for arginine (R) at position 100 in the mature NGF (NGF^{R100W}) (Einarsdottir et al., 2004). Previous clinical studies have shown that HSAN V patients that were homozygous for NGF^{R100W} mutation had earlier onset and exhibited more severe clinical manifestations than heterozygous carriers (de Andrade et al., 2008; Einarsdottir et al., 2004; Minde et al., 2004). Homozygous patients also reported an inability to detect painful stimuli since birth, which prevents them from feeling pain from heat, bone fractures and joints and leads to destroyed joints in childhood. Sural nerve biopsy with morphometric analysis from homozygous patients further demonstrated a moderate loss of myelinated Aδ fibers and a severer reduction of unmyelinated C fibers (Minde et al., 2004). These HSAN V patients suffer from severe loss of pain perception but retain normal cognitive function (Capsoni, 2014; Einarsdottir et al., 2004; Minde et al., 2009), suggesting that the NGF^{R100W} mutation may result in selective loss of pain-inducing function, while retaining its trophic function (Capsoni, 2014; Capsoni et al., 2011; Sung et al., 2018, 2019; Testa et al., 2019b).

To better define the mechanisms of NGF^{R100W} and to study the functional impact of NGF^{R100W} on development, we and others have generated mouse models using the knockin technology(Testa et al., 2019a,b; Yang et al., 2018). Testa and colleagues knocked in a human NGF allele carrying the R100W mutation into the mouse genome (Testa et al., 2019a, b). Initial characterization of this model has shown that cholinergic neurons was increased specifically in the striatum in the homozygous mutant mice (Testa et al., 2019a); Structurally, the heterozygous mutant mice showed no changes in the different DRG subpopulations while skin innervation was reduced (Testa et al., 2019b). The heterozygous mutant mice developed a deficit in nociception while showing no learning or memory deficits (Testa et al., 2019b). Given that mouse and human NGF are highly conserved in both structure and function, these studies have made significant contribution toward our understanding of NGF function and potential pathogenic mechanism(s) of HASN V.

However, mature NGF amino acid sequences from mouse and human have a 13/121 (10.74 %) difference (see Fig. 3A) (Paoletti et al.,

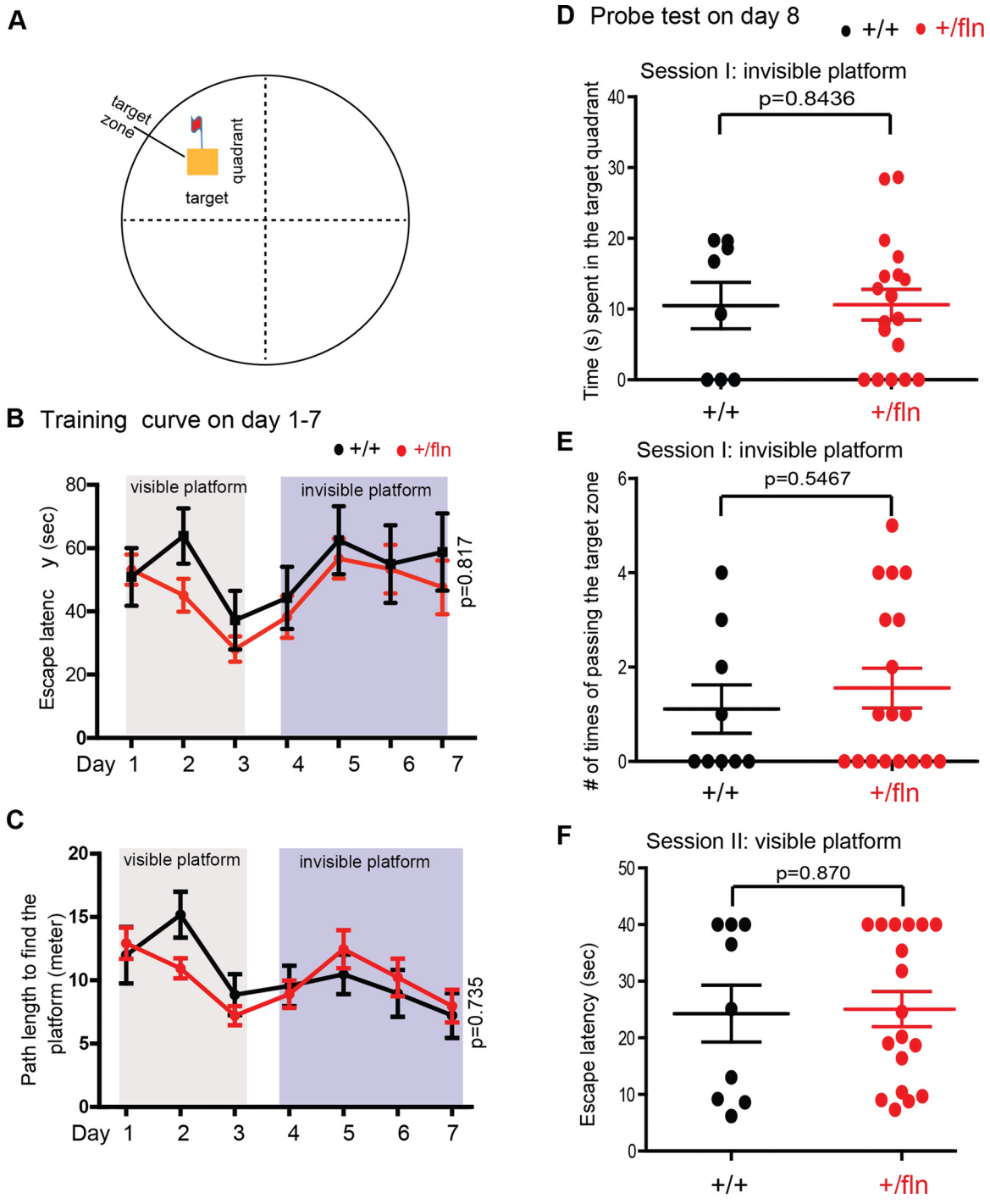

Fig. 7. The +/fln mutant mice show no significant deficit in Morris water maze test. (A) Diagram of Morris water maze. The test mice (18 month–old) were first trained to find a platform with a visible flag on days 1 to 3 and then a submerged hidden platform on days 4 to 7. The time (B) and path length (C) to find the platform was recorded. On day 8 of probe test, the platform was removed in session I. Times spent by mice in the target quadrant (D) and # passing of the target zone (E) were recorded. In session II, the visible platform was placed back and the latency time (F) was recorded. All data are presented as Mean ± SEM. p = 0.817 for B and p = 0.735 for C. p values were calculated by two-way ANOVA; p values for D, E, F by unpaired t test. +/+: n = 9, +/fln: n = 18.

2015). Furthermore, the mouse and human TrkA d5 domain have a difference of 11/102 in amino acid residues (see Fig. 3B) (Paoletti et al., 2015). As such, an elegant study from Dr. Cattaneo's group has previously demonstrated that mouse NGF and human NGF displayed strikingly differences in the structural, functional and biological differences (Paoletti et al., 2015). Therefore, Dr. Cattaneo and colleagues have correctly cautioned that "special care must be taken in performing experiments with cross-species systems in the laboratory practice, in developing immunoassays, in clinical trials and in pharmacological treatments"(Paoletti et al., 2015).

These potential complications are unlikely an issue in our study since our mouse model harbored only the mouse NGF allele with the R100W mutation (Yang et al., 2018). Nevertheless, our current study has yielded results consistent with Testa and colleagues (Testa et al., 2019a,b), we found that the mouse NGF^{R100W} knockin model recapitulates the clinical manifestation of HSAN V; the homozygotes showed severe sensory loss both structurally and functionally at as early as P0, while the heterozygotes developed progressive peripheral

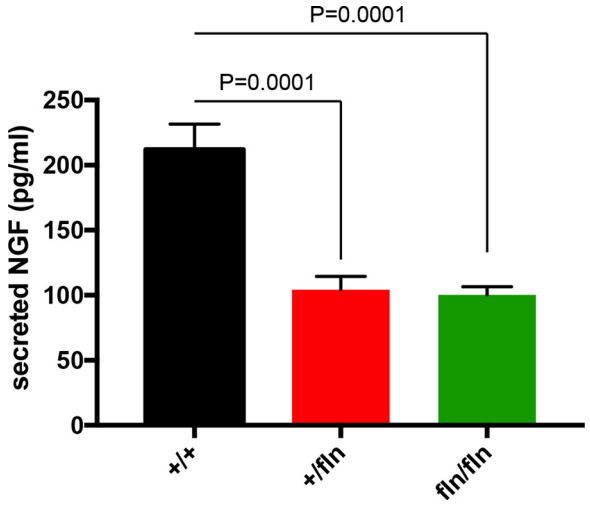

Fig. 8. NGF secretion is decreased in +/fln and fln/fln mouse embryonic fibroblasts. NGF protein content in media was measured by ELISA. Data from NGF ELISA was presented as Mean ± SEM; n = 6 for each experimental group. p values were calculated by Dunnett's multiple comparisons test.

sensory neuropathy. Importantly, our tests have revealed that the heterozygotes did not show significant impairment of CNS function. Therefore, together with the Testa model (Testa et al., 2019a,b), our mouse model will serve as an important tool in not only understanding the pathogenesis of HSAN V, but also will be instrumental in uncoupling the nociceptive function from trophic function of NGF.

The NGF^{R100W} homozygotes had significant fewer numbers of small CGRP-positive neurons in their DRGs as well as PGP9.5-IENFs in their skin at birth. They frequently failed to survive to adulthood. The ones that did survive to 6–8 weeks displayed significant deficits in sensing thermal stimuli, a result that appeared to be consistent with the lack of sensory fibers and neurons in these mice. In many ways, our NGF^{R100W} homozygotes resemble both the TrkA knockout (Smeyne et al., 1994) and the NGF knockout ($NGF^{-/-}$) mice in their severe sensory phenotypic presentations (Crowley et al., 1994); The NGF knockout mice also failed to respond to noxious mechanical stimuli with profound cell loss of small neurons in their DRGs (Crowley et al., 1994). The similarities between NGF^{R100W} homozygotes and $NGF^{-/-}$ may suggest that the structural and functional deficits in the NGF^{R100W} homozygotes are likely resulted from NGF deficiency. Indeed, Testa and colleagues have demonstrated that treating newborn homozygous NGFR100W/R100W pups with wt NGF improved their survival in their human NGFR100W knockin model (Testa et al., 2019a). Additional experiments will be needed to confirm if this is indeed the case in our model.

Unlike the homozygotes with early onset of peripheral deficits, NGF^{R100W} heterozygotes did not appear to suffer from any developmental deficits at birth and at 2 months of age. Starting at 9 months, these mice began to show structural degeneration of small CGRP-positive neurons in their DRGs as well as IENFs in their skins. Not surprisingly, they began to develop peripheral sensory deficits. At 18 months of age, these mice showed worsening deficits both structurally and functionally. Therefore, similar to HSAN V patients with a late onset disease, NGF^{R100W} homozygotes show a progressive degeneration of the peripheral sensory system. Intriguingly, the impact of NGF^{R100W} seems to be restricted to the peripheral system, as our examination of the CNS did not identify significant changes both functionally and structurally in these mice, consistent with previous studies (Testa et al., 2019a, b).

In some aspects, NGF^{R100W} heterozygotes exhibit phenotypes similar to the NGF hemizygotes ($NGF^{+/-}$), in that these $NGF^{+/-}$ mice also showed a moderate reduction of sensory fiber in the skin and CGRP-immunoreactive sensory neurons in the lumbar DRGs (Crowley et al., 1994). Furthermore, these $NGF^{+/-}$ mice displayed decreased responsiveness to pain (Crowley et al., 1994). However, some significant differences exist between the +/fln mice and the $NGF^{+/-}$ mice; The $NGF^{+/-}$ mice had significantly fewer ChAT-immunoreactive neurons within the medial septal and AChE-positive fibers in CA1, CA3 and dentate gyrus regions of the hippocampal formation (Chen et al., 1997). In addition, $NGF^{+/-}$ mice showed significant acquisition and retention deficits in the water maze test (Chen et al., 1997). Whereas in the present study, we did not detect any significant neuronal loss in the hippocampus and media septum of the +/fln mice even at the advance age of 18-month old. Furthermore, in a battery of behavioral tests for CNS function ranging from spontaneous alternation, spatial memory, novel object recognition, sociability interaction test and anxiety tests (marble test and light-dark shuttle box test), we did not detect any differences between the +/fln mice and age-matched +/+ littermate controls. These results demonstrate that NGF^{R100W} show no apparent dysfunction in CNS, an important distinction from the $TrkA^{-/-}$ (Smeyne et al., 1994) and the $NGF^{+/-}$ mice (Chen et al., 1997). Our data suggest that the NGF^{R100W} allele in the +/fln mice may retain a certain level of trophic function to support the development and function of the brain, while this level of trophic support of the NGF^{R100W} allele is not sufficient in maitaining the structure and function of the peripheral sensory neurons. Taken together, our findings have demonstrated that the +/fln mice have adult onset, as in HSAN V heterozygous patients, and develop progressive nociceptive deficits and peripheral neuropathy.

The late onset and phenotypic presentations observed in the +/fln mice are largely in agreement with human HSAN V conditions as well as with the mutant mice investigated by Testa and colleagues (Testa et al., 2019a, b). The HSAN V heterozygous patients usually had adult onset and a milder progressive course (Einarsdottir et al., 2004; Minde et al., 2004). For example, one 75-year-old heterozygous carriers underwent a painless fracture of his right ankle at age 48 and 8 years later he developed advanced osteoarthritis in both talocrural joints and left knee with only slight pain (Minde et al., 2004). The sural nerve biopsies also showed moderate loss of thin myelinated fibers and a severer reduction of unmyelinated fibers. Therefore, the +/fln are an ideal model for studying HSAN V disease.

Recently, human genetic study has linked another case of HSAN V in a consanguineous Arab family to a homozygous mutation in the NGF gene, c.[680C > A] + [681_682delGG] (Carvalho et al., 2011). The mutations reside in the "CGG" codon at the 680–682 position: 'C' was changed to 'A' with "GG" being deleted, resulting in the terminal 15 amino acids of NGF being replaced with a novel 43 amino acid terminal sequence (NGF^{V232fs})(Carvalho et al., 2011). Clinical manifestations of these patients are similar to HSAN IV associated with mutations in TrkA (Indo, 2002), in that they were completely unable to perceive pain, did not sweat, could not discriminate temperature, and had a chronic immunodeficiency (Capsoni, 2014; Carvalho et al., 2011; Indo, 2002). In addition, like HSAN IV patients, these Arabian patients suffered from intellectually disabled (Capsoni, 2014; Carvalho et al., 2011). Therefore, in the case of NGF^{V232fs}, it is possible that the mutation results in reduced binding and activation of NGF to TrkA; Alternatively, the mutation impairs the processing of $proNGF^{V232fs}$ and reduces its secretion as demonstrated in in vitro experiments (Carvalho et al., 2011). In either case, TrkA-mediated signaling is expected to be diminished. As a consequence, the development and function of both PNS and CNS are affected.

That the impact of the NGF^{R100W} mutation is largely restricted to PNS function points to some clear distinctions from the NGF^{V232fs} mutation. It is also possible that the NGF^{R100W} mutation has resulted in changes in the processing, secretion and stability of NGF, albeit to a much lesser degree than for NGF^{V232fs}. Our study showed that NGF secretion was reduced to a comparable level in fibroblast cells from both homozygous and heterozygous mutant mice in comparison to wt mice. Yet, the severity of morphological and behavioral defects between the two genotypes was significantly different. It has been well

established that NGF needs to form dimers to be active biologically. We speculate that there may be due to a difference in the bioactivity between different NGF dimers potentially formed in the homozygotes and heterozygotes; The homozygotes have only NGF dimers that comprise of two R100W mutant NGF molecules (R100W:R100W), whereas in the heterozygotes, in addition to the R100W:R100W dimer, both wt:wt and wt:R100W dimers also exist. It is likely the R100W:R100W dimers exhibits less bioactivity than either wt:wt or wt:R100W dimers, thus contributing to the different severity of morphological and behavioral defects between the homozygous and the heterozygous mutant mice.

The NGF^{R100W} mutation is located in a highly conserved region that is important for binding and activating $p75^{NTR}$ (Einarsdottir et al., 2004). Surface Plasmon Resonance analyses demonstrated that NGF^{R100W} mutation selectively abolishes NGF binding to $p75^{NTR}$, while the affinity for TrkA receptor is retained (Capsoni et al., 2011; Covaceuszach et al., 2010). Therefore, it is likely that the loss of $p75^{NTR}$-mediated signaling in NGF^{R100W} may contribute to impairment of peripheral function in sensing pain. Indeed, increasing evidence supports the notion that $p75^{NTR}$ involved in NGF-induced hyperalgesia (Capsoni, 2014; Capsoni et al., 2011; Sung et al., 2018, 2019). Intrathecal administration of antisense oligodeoxynucleotides specific for $p75^{NTR}$ into neuropathic pain model, which reduced its expression in the DRG, attenuated thermal hyperalgesia and mechanical allodynia after nerve injury (Obata et al., 2004). Besides, application of $p75^{NTR}$ blocking antibody inhibited the sensitizing action of NGF to increase the number of action potentials (Zhang and Nicol, 2004) and suppressed mechanical allodynia from crushed sciatic nerve (Fukui et al., 2010). Moreover, administration of neutralizing antibody to $p75^{NTR}$ blocked hyperalgesia arising from an intraplantar injection of NGF (Watanabe et al., 2008). Furthermore, the effect of $p75^{NTR}$ knockout animal mice seemed to be restricted to the sensory nervous system (Lee et al., 1992). This indicates that $p75^{NTR}$ mainly mediate signaling to induce hyperalgesia.

In summary, we have generated a NGF^{R100W} knockin mouse model for studying HSAN V. Our studies have demonstrated that the NGF^{R100W} knockin mice suffer structural and functional degeneration of the peripheral sensory system as in HSAN V patients. Furthermore, also as in HSAN V patients, the NGF mutant mice show no significant cognitive deficits, an important feature that distinguishes NGF^{R100W}-HSAN V from both NGF^{V232fs}-HSAN V and HSAN IV associated with TrkA mutations. Together with the Testa model (Testa et al., 2019a, b), this mouse model will provide exciting opportunities to further define the disease mechanisms for HSAN V. More importantly, the unique NGF^{R100W} mouse model will facilitate studies to define how NGF^{R100W} retains its trophic signal while the nociceptive function is lost in NGF^{R100W}.

Author contributions

WY, KS, JD and CW designed the study; WY. KS, WX, MJR, ACW, SAS, SF, RKU, SXD, BCG, XO, JR performed the experiments. WY, KS, KJ, NC, RR, JD and CW wrote the paper. All authors discussed the results and commented on the manuscript.

Acknowledgements

We would like to thank Dr William C Mobley for advice and all members of our laboratory for comments and suggestions. We also thank Ms Pauline Hu and Dr. Olga Prikhodko for technical assistance; We would also like Ms. Angela Zeng, Mr. Simon Kim for helping with quantitation of IENFs; This research was supported by grants from: China Postdoctoral Science Foundation (No.2019M662987) to WY; UCSD T32 Neuroplasticity Training Grant to KS; National Natural Science Foundation of China (No.81600920) to WX; NIH AG-039736 to CGJ; NIH NS081082 to NC; ; NIHAG051848, BX003040, AG051839, AG018440 toRAR.Larry L Hillblom Foundation, Tau Consortium and UCSD P50 Pilot Grants to CW.

Appendix A. Supplementary data

Supplementary material related to this article can be found, in the online version, at doi:https://doi.org/10.1016/j.pneurobio.2020.101886.

References

Apfel, S.C., 2002. Nerve growth factor for the treatment of diabetic neuropathy: what went wrong, what went right, and what does the future hold? Int. Rev. Neurobiol. 50, 393–413.
Apfel, S.C., Kessler, J.A., Adornato, B.T., Litchy, W.J., Sanders, C., Rask, C.A., 1998. Recombinant human nerve growth factor in the treatment of diabetic polyneuropathy. NGF Study Group. Neurology 51, 695–702.
Blesch, A., Tuszynski, M., 1995. Ex vivo gene therapy for Alzheimer's disease and spinal cord injury. Clin. Neurosci. 3, 268–274.
Bothwell, M., 1995. Functional interactions of neurotrophins and neurotrophin receptors. Annu. Rev. Neurosci. 18, 223–253.
Capsoni, S., 2014. From genes to pain: nerve growth factor and hereditary sensory and autonomic neuropathy type V. Eur. J. Neurosci. 39, 392–400.
Capsoni, S., Covaceuszach, S., Marinelli, S., Ceci, M., Bernardo, A., Minghetti, L., Ugolini, G., Pavone, F., Cattaneo, A., 2011. Taking pain out of NGF: a "painless" NGF mutant, linked to hereditary sensory autonomic neuropathy type V, with full neurotrophic activity. PLoS One 6, e17321.
Carpenter, A.C., Saborido, T.P., Stanwood, G.D., 2012. Development of hyperactivity and anxiety responses in dopamine transporter-deficient mice. Dev. Neurosci. 34, 250–257.
Carvalho, O.P., Thornton, G.K., Hertecant, J., Houlden, H., Nicholas, A.K., Cox, J.J., Rielly, M., Al-Gazali, L., Woods, C.G., 2011. A novel NGF mutation clarifies the molecular mechanism and extends the phenotypic spectrum of the HSAN5 neuropathy. J. Med. Genet. 48, 131–135.
Casaccia-Bonnefil, P., Kong, H., Chao, M.V., 1998. Neurotrophins: the biological paradox of survival factors eliciting apoptosis. Cell Death Differ. 5, 357–364.
Cattaneo, A., Capsoni, S., 2019. Painless Nerve Growth Factor: a TrkA biased agonist mediating a broad neuroprotection via its actions on microglia cells. Pharmacol. Res. 139, 17–25.
Chao, M.V., 2003. Neurotrophins and their receptors: a convergence point for many signalling pathways. Nat. Rev. Neurosci. 4, 299–309.
Chao, M.V., Hempstead, B.L., 1995. p75 and Trk: a two-receptor system. Trends Neurosci. 18, 321–326.
Chen, K.S., Nishimura, M.C., Armanini, M.P., Crowley, C., Spencer, S.D., Phillips, H.S., 1997. Disruption of a single allele of the nerve growth factor gene results in atrophy of basal forebrain cholinergic neurons and memory deficits. J. neurosci. Off. J. Soc. Neurosci. 17, 7288–7296.
Chuang, H.H., Prescott, E.D., Kong, H., Shields, S., Jordt, S.E., Basbaum, A.I., Chao, M.V., Julius, D., 2001. Bradykinin and nerve growth factor release the capsaicin receptor from PtdIns(4,5)P2-mediated inhibition. Nature 411, 957–962.
Conover, J.C., Yancopoulos, G.D., 1997. Neurotrophin regulation of the developing nervous system: analyses of knockout mice. Rev. Neurosci. 8, 13–27.
Covaceuszach, S., Capsoni, S., Marinelli, S., Pavone, F., Ceci, M., Ugolini, G., Vignone, D., Amato, G., Paoletti, F., Lamba, D., et al., 2010. In vitro receptor binding properties of a "painless" NGF mutein, linked to hereditary sensory autonomic neuropathy type V. Biochem. Biophys. Res. Commun. 391, 824–829.
Crowley, C., Spencer, S.D., Nishimura, M.C., Chen, K.S., Pitts-Meek, S., Armanini, M.P., Ling, L.H., McMahon, S.B., Shelton, D.L., Levinson, A.D., et al., 1994. Mice lacking nerve growth factor display perinatal loss of sensory and sympathetic neurons yet develop basal forebrain cholinergic neurons. Cell 76, 1001–1011.
Cuello, A.C., Bruno, M.A., Allard, S., Leon, W., Iulita, M.F., 2010. Cholinergic involvement in Alzheimer's disease. A link with NGF maturation and degradation. J. Mol. Neurosci. 40, 230–235.
de Andrade, D.C., Baudic, S., Attal, N., Rodrigues, C.L., Caramelli, P., Lino, A.M., Marchiori, P.E., Okada, M., Scaff, M., Bouhassira, D., et al., 2008. Beyond neuropathy in hereditary sensory and autonomic neuropathy type V: cognitive evaluation. Eur. J. Neurol. 15, 712–719.
Einarsdottir, E., Carlsson, A., Minde, J., Toolanen, G., Svensson, O., Solders, G., Holmgren, G., Holmberg, D., Holmberg, M., 2004. A mutation in the nerve growth factor beta gene (NGFB) causes loss of pain perception. Hum. Mol. Genet. 13, 799–805.
Eriksdotter Jonhagen, M., Nordberg, A., Amberla, K., Backman, L., Ebendal, T., Meyerson, B., Olson, L., Seiger Shigeta, M., Theodorsson, E., et al., 1998. Intracerebroventricular infusion of nerve growth factor in three patients with Alzheimer's disease. Dement. Geriatr. Cogn. Disord. 9, 246–257.
Fukui, Y., Ohtori, S., Yamashita, M., Yamauchi, K., Inoue, G., Suzuki, M., Orita, S., Eguchi, Y., Ochiai, N., Kishida, S., et al., 2010. Low affinity NGF receptor (p75 neurotrophin receptor) inhibitory antibody reduces pain behavior and CGRP expression in DRG in the mouse sciatic nerve crush model. J. Orthop. Res. 28, 279–283.
Haga, N., Kubota, M., Miwa, Z., Japanese Research Group on Congenital Insensitivity to, P., 2015. Hereditary sensory and autonomic neuropathy types IV and V in Japan. Pediatr. Int. 57, 30–36.
Hamburger, V., Levi-Montalcini, R., 1949. Proliferation, differentiation and degeneration in the spinal ganglia of the chick embryo under normal and experimental conditions.

J. Exp. Zool. 111, 457–501.
Hefti, F., 1994. Development of effective therapy for Alzheimer's disease based on neurotrophic factors. Neurobiol. Aging 15 (Suppl 2), S193–194.
Hellweg, R., Hartung, H.D., 1990. Endogenous levels of nerve growth factor (NGF) are altered in experimental diabetes mellitus: a possible role for NGF in the pathogenesis of diabetic neuropathy. J. Neurosci. Res. 26, 258–267.
Heredia, L., Torrente, M., Colomina, M.T., Domingo, J.L., 2014. Assessing anxiety in C57BL/6J mice: a pharmacological characterization of the open-field and light/dark tests. J. Pharmacol. Toxicol. Methods 69, 108–114.
Huang, E.J., Reichardt, L.F., 2001. Neurotrophins: roles in neuronal development and function. Annu. Rev. Neurosci. 24, 677–736.
Indo, Y., 2001. Molecular basis of congenital insensitivity to pain with anhidrosis (CIPA): mutations and polymorphisms in TRKA (NTRK1) gene encoding the receptor tyrosine kinase for nerve growth factor. Hum. Mutat. 18, 462–471.
Indo, Y., 2002. Genetics of congenital insensitivity to pain with anhidrosis (CIPA) or hereditary sensory and autonomic neuropathy type IV. Clinical, biological and molecular aspects of mutations in TRKA(NTRK1) gene encoding the receptor tyrosine kinase for nerve growth factor. Clin. Auton. Res. 12 (Suppl 1), I20–32.
Kaidanovich-Beilin, O., Lipina, T., Vukobradovic, I., Roder, J., Woodgett, J.R., 2011. Assessment of social interaction behaviors. J. Vis. Exp. 48, 273. https://doi.org/10.3791/2473.
Kaplan, D.R., Miller, F.D., 1997. Signal transduction by the neurotrophin receptors. Curr. Opin. Cell Biol. 9, 213–221.
Kew, J.N., Smith, D.W., Sofroniew, M.V., 1996. Nerve growth factor withdrawal induces the apoptotic death of developing septal cholinergic neurons in vitro: protection by cyclic AMP analogue and high potassium. Neuroscience 70, 329–339.
Khodorova, A., Nicol, G.D., Strichartz, G., 2013. The p75NTR signaling cascade mediates mechanical hyperalgesia induced by nerve growth factor injected into the rat hind paw. Neuroscience 254, 312–323.
Kleschevnikov, A.M., Yu, J., Kim, J., Lysenko, L.V., Zeng, Z., Yu, Y.E., Mobley, W.C., 2017. Evidence that increased Kcnj6 gene dose is necessary for deficits in behavior and dentate gyrus synaptic plasticity in the Ts65Dn mouse model of Down syndrome. Neurobiol. Dis. 103, 1–10.
Knusel, B., Gao, H., 1996. Neurotrophins and Alzheimer's disease: beyond the cholinergic neurons. Life Sci. 58, 2019–2027.
Koliatsos, V.E., 1996. Biological therapies for Alzheimer's disease: focus on trophic factors. Crit. Rev. Neurobiol. 10, 205–238.
Larsson, E., Kuma, R., Norberg, A., Minde, J., Holmberg, M., 2009. Nerve growth factor R221W responsible for insensitivity to pain is defectively processed and accumulates as proNGF. Neurobiol. Dis. 33, 221–228.
Lee, K.F., Li, E., Huber, L.J., Landis, S.C., Sharpe, A.H., Chao, M.V., Jaenisch, R., 1992. Targeted mutation of the gene encoding the low affinity NGF receptor p75 leads to deficits in the peripheral sensory nervous system. Cell 69, 737–749.
Lehmann, M., Fournier, A., Selles-Navarro, I., Dergham, P., Sebok, A., Leclerc, N., Tigyi, G., McKerracher, L., 1999. Inactivation of Rho signaling pathway promotes CNS axon regeneration. J. Neurosci. 19, 7537–7547.
Lein, B., 1995. Potential therapy for painful neuropathy. PI Perspect. 11.
Levi-Montalcini, R., 1987. The nerve growth factor 35 years later. Science 237, 1154–1162.
Levi-Montalcini, R., 2004. The nerve growth factor and the neuroscience chess board. Prog. Brain Res. 146, 525–527.
Levi-Montalcini, R., Hamburger, V., 1951. Selective growth stimulating effects of mouse sarcoma on the sensory and sympathetic nervous system of the chick embryo. J. Exp. Zool. 116, 321–361.
Levi-Montalcini, R., Dal Toso, R., della Valle, F., Skaper, S.D., Leon, A., 1995. Update of the NGF saga. J. Neurol. Sci. 130, 119–127.
Lewin, G.R., Mendell, L.M., 1993. Nerve growth factor and nociception. Trends Neurosci. 16, 353–359.
Lewin, G.R., Ritter, A.M., Mendell, L.M., 1993. Nerve growth factor-induced hyperalgesia in the neonatal and adult rat. J. Neurosci. 13, 2136–2148.
Li, X., Jope, R.S., 1995. Selective inhibition of the expression of signal transduction proteins by lithium in nerve growth factor-differentiated PC12 cells. J. Neurochem. 65, 2500–2508.
Li, C.L., Li, K.C., Wu, D., Chen, Y., Luo, H., Zhao, J.R., Wang, S.S., Sun, M.M., Lu, Y.J., Zhong, Y.Q., et al., 2016. Somatosensory neuron types identified by high-coverage single-cell RNA-sequencing and functional heterogeneity. Cell Res. 26, 967.
Lueptow, L.M., 2017. Novel object recognition test for the investigation of learning and memory in mice. J. Vis. Exp. 126, 55718. https://doi.org/10.3791/55718.
McArthur, J.C., Yiannoutsos, C., Simpson, D.M., Adornato, B.T., Singer, E.J., Hollander, H., Marra, C., Rubin, M., Cohen, B.A., Tucker, T., et al., 2000. A phase II trial of nerve growth factor for sensory neuropathy associated with HIV infection. AIDS Clinical Trials Group Team 291. Neurology 54, 1080–1088.
Meyer, R.A., Campbell, J.N., Raja, S.N., 2006. Peripheral mechanisms of cutaneous nociception. In: McMahon, K.Me. (Ed.), Wall and Melzack's Textbook of Pain. Elsevier, pp. 3–34 SB.
Minde, J.K., 2006. Norrbottnian congenital insensitivity to pain. Acta Orthop. Suppl. 77, 2–32.
Minde, J., Toolanen, G., Andersson, T., Nennesmo, I., Remahl, I.N., Svensson, O., Solders, G., 2004. Familial insensitivity to pain (HSAN V) and a mutation in the NGFB gene. A neurophysiological and pathological study. Muscle Nerve 30, 752–760.
Minde, J., Svensson, O., Holmberg, M., Solders, G., Toolanen, G., 2006. Orthopedic aspects of familial insensitivity to pain due to a novel nerve growth factor beta mutation. Acta Orthop. 77, 198–202.
Minde, J., Andersson, T., Fulford, M., Aguirre, M., Nennesmo, I., Remahl, I.N., Svensson, O., Holmberg, M., Toolanen, G., Solders, G., 2009. A novel NGFB point mutation: a phenotype study of heterozygous patients. J. Neurol. Neurosurg. Psychiatr. 80, 188–195.
Mobley, W.C., Rutkowski, J.L., Tennekoon, G.I., Gemski, J., Buchanan, K., Johnston, M.V., 1986. Nerve growth factor increases choline acetyltransferase activity in developing basal forebrain neurons. Brain Res. 387, 53–62.
Morrison, I., Loken, L.S., Minde, J., Wessberg, J., Perini, I., Nennesmo, I., Olausson, H., 2011. Reduced C-afferent fibre density affects perceived pleasantness and empathy for touch. Brain 134, 1116–1126.
Mufson, E.J., Counts, S.E., Perez, S.E., Ginsberg, S.D., 2008. Cholinergic system during the progression of Alzheimer's disease: therapeutic implications. Expert Rev. Neurother. 8, 1703–1718.
Nykjaer, A., Willnow, T.E., Petersen, C.M., 2005. p75NTR–live or let die. Curr. Opin. Neurobiol. 15, 49–57.
Obata, K., Yamanaka, H., Kobayashi, K., Dai, Y., Mizushima, T., Katsura, H., Fukuoka, T., Tokunaga, A., Noguchi, K., 2004. Role of mitogen-activated protein kinase activation in injured and intact primary afferent neurons for mechanical and heat hypersensitivity after spinal nerve ligation. J. Neurosci. 24, 10211–10222.
Olson, L., 1993. NGF and the treatment of Alzheimer's disease. Exp. Neurol. 124, 5–15.
Paoletti, F., Malerba, F., Ercole, B.B., Lamba, D., Cattaneo, A., 2015. A comparative analysis of the structural, functional and biological differences between mouse and human nerve growth factor. Biochim. Biophys. Acta 1854, 187–197.
Perini, I., Tavakoli, M., Marshall, A., Minde, J., Morrison, I., 2016. Rare human nerve growth factor-beta mutation reveals relationship between C-afferent density and acute pain evaluation. J. Neurophysiol. 116, 425–430.
Pezet, S., McMahon, S.B., 2006. Neurotrophins: mediators and modulators of pain. Annu. Rev. Neurosci. 29, 507–538.
Pradat, P.F., 2003. [Treatment of peripheral neuropathies with neutrotrophic factors: animal models and clinical trials]. Rev Neurol (Paris) 159, 147–161.
Price, D.D., 2000. Psychological and neural mechanisms of the affective dimension of pain. Science 288, 1769–1772.
Quasthoff, S., Hartung, H.P., 2001. [Nerve growth factor (NGF) in treatment of diabetic polyneuropathy. One hope less?]. Nervenarzt 72, 456–459.
Rafii, M.S., Baumann, T.L., Bakay, R.A., Ostrove, J.M., Siffert, J., Fleisher, A.S., Herzog, C.D., Barba, D., Pay, M., Salmon, D.P., et al., 2014. A phase1 study of stereotactic gene delivery of AAV2-NGF for Alzheimer's disease. Alzheimer's & dementia: J. Alzheimer's Assoc. 10, 571–581.
Rask, C.A., 1999. Biological actions of nerve growth factor in the peripheral nervous system. Eur. Neurol. 41 (Suppl 1), 14–19.
Roux, P.P., Colicos, M.A., Barker, P.A., Kennedy, T.E., 1999. p75 neurotrophin receptor expression is induced in apoptotic neurons after seizure. J. Neurosci. 19, 6887–6896.
Sagafos, D., Kleggetveit, I.P., Helas, T., Schmidt, R., Minde, J., Namer, B., Schmelz, M., Jorum, E., 2016. Single-fiber recordings of nociceptive fibers in patients with HSAN type V with congenital insensitivity to pain. Clin. J. Pain 32, 636–642.
Schifitto, G., Yiannoutsos, C., Simpson, D.M., Adornato, B.T., Singer, E.J., Hollander, H., Marra, C.M., Rubin, M., Cohen, B.A., Tucker, T., et al., 2001. Long-term treatment with recombinant nerve growth factor for HIV-associated sensory neuropathy. Neurology 57, 1313–1316.
Schindowski, K., Belarbi, K., Buee, L., 2008. Neurotrophic factors in Alzheimer's disease: role of axonal transport. Genes Brain Behav. 7 (Suppl 1), 43–56.
Schulte-Herbruggen, O., Jockers-Scherubl, M.C., Hellweg, R., 2008. Neurotrophins: from pathophysiology to treatment in Alzheimer's disease. Curr. Alzheimer Res. 5, 38–44.
Scott, S.A., Crutcher, K.A., 1994. Nerve growth factor and Alzheimer's disease. Rev. Neurosci. 5, 179–211.
Smeyne, R.J., Klein, R., Schnapp, A., Long, L.K., Bryant, S., Lewin, A., Lira, S.A., Barbacid, M., 1994. Severe sensory and sympathetic neuropathies in mice carrying a disrupted Trk/NGF receptor gene. Nature 368, 246–249.
Spencer, B., Valera, E., Rockenstein, E., Overk, C., Mante, M., Adame, A., Zago, W., Seubert, P., Barbour, R., Schenk, D., et al., 2017. Anti-alpha-synuclein immunotherapy reduces alpha-synuclein propagation in the axon and degeneration in a combined viral vector and transgenic model of synucleinopathy. Acta Neuropathol. Commun. 5, 7.
Sung, K., Ferrari, L.F., Yang, W., Chung, C., Zhao, X., Gu, Y., Lin, S., Zhang, K., Cui, B., Pearn, M.L., et al., 2018. Swedish nerve growth factor mutation (NGF(R100W)) defines a role for TrkA and p75(NTR) in nociception. J. Neurosci. 38, 3394–3413.
Sung, K., Yang, W., Wu, C., 2019. Uncoupling neurotrophic function from nociception of nerve growth factor: what can be learned from a rare human disease? Neural Regen. Res. 14, 570–573.
Svendsen, C.N., Kew, J.N., Staley, K., Sofroniew, M.V., 1994. Death of developing septal cholinergic neurons following NGF withdrawal in vitro: protection by protein synthesis inhibition. J. Neurosci. 14, 75–87.
Testa, G., Calvello, M., Cattaneo, A., Capsoni, S., 2019a. Cholinergic striatal neurons are increased in HSAN V homozygous mice despite reduced NGF bioavailability. Biochem. Biophys. Res. Commun. 509, 763–766.
Testa, G., Mainardi, M., Morelli, C., Olimpico, F., Pancrazi, L., Petrella, C., Severini, C., Florio, R., Malerba, F., Stefanov, A., et al., 2019b. The NGF(R100W) Mutation Specifically Impairs Nociception without Affecting Cognitive Performance in a Mouse Model of Hereditary Sensory and Autonomic Neuropathy Type V. J. Neurosci. 39, 9702–9715.
Thomas, A., Burant, A., Bui, N., Graham, D., Yuva-Paylor, L.A., Paylor, R., 2009. Marble burying reflects a repetitive and perseverative behavior more than novelty-induced anxiety. Psychopharmacology (Berl.) 204, 361–373.
Unger, J.W., Klitzsch, T., Pera, S., Reiter, R., 1998. Nerve growth factor (NGF) and diabetic neuropathy in the rat: morphological investigations of the sural nerve, dorsal root ganglion, and spinal cord. Exp. Neurol. 153, 23–34.
Usoskin, D., Furlan, A., Islam, S., Abdo, H., Lönnerberg, P., Lou, D., Hjerling-Leffler, J., Haeggström, J., Kharchenko, O., Kharchenko, P.V., et al., 2015. Unbiased classification of sensory neuron types by large-scale single-cell RNA sequencing. Nat.

Neurosci. 18, 145–153.
Walwyn, W.M., Matsuka, Y., Arai, D., Bloom, D.C., Lam, H., Tran, C., Spigelman, I., Maidment, N.T., 2006. HSV-1-mediated NGF delivery delays nociceptive deficits in a genetic model of diabetic neuropathy. Exp. Neurol. 198, 260–270.
Watanabe, T., Ito, T., Inoue, G., Ohtori, S., Kitajo, K., Doya, H., Takahashi, K., Yamashita, T., 2008. The p75 receptor is associated with inflammatory thermal hypersensitivity. J. Neurosci. Res. 86, 3566–3574.
Williams, B.J., Eriksdotter-Jonhagen, M., Granholm, A.C., 2006. Nerve growth factor in treatment and pathogenesis of Alzheimer's disease. Prog. Neurobiol. 80, 114–128.
Willis, W.D., 2004. Sensory receptors and peripheral nerves. In: Willis, C.Re. (Ed.), In Sensory Mechanisms of the Spinal Cord. Kluwer Academic/Plenum Publishres, New York, Boston, USA; Dordrecht, London, UK; Moscow, Russia, pp. 19–87 C.R.W.D., ed.
Yang, W., Sung, K., Zhou, F., Xu, W., Rissman, R.A., Ding, J., Wu, C., 2018. Targeted mutation (R100W) of the gene encoding NGF leads to deficits in the peripheral sensory nervous system. Front. Aging Neurosci. 10, 373.
Zhang, Y.H., Nicol, G.D., 2004. NGF-mediated sensitization of the excitability of rat sensory neurons is prevented by a blocking antibody to the p75 neurotrophin receptor. Neurosci. Lett. 366, 187–192.
Zhang, Y.H., Vasko, M.R., Nicol, G.D., 2002. Ceramide, a putative second messenger for nerve growth factor, modulates the TTX-resistant Na(+) current and delayed rectifier K(+) current in rat sensory neurons. J Physiol 544, 385–402.
Zhang, Y.H., Vasko, M.R., Nicol, G.D., 2006. Intracellular sphingosine 1-phosphate mediates the increased excitability produced by nerve growth factor in rat sensory neurons. J Physiol 575, 101–113.
Zhou, X.F., Rush, R.A., McLachlan, E.M., 1996. Differential expression of the p75 nerve growth factor receptor in glia and neurons of the rat dorsal root ganglia after peripheral nerve transection. J. Neurosci. 16, 2901–2911.